

# **Polycrystalline carbon nanotubes for hydrogen storage using molecular dynamics simulations**

**M.Tech. Thesis**

By

**ANKIT KUMAR**

**1802103023**



Discipline of Mechanical Engineering  
**Indian Institute of Technology Indore**  
DEC 2020

# **Polycrystalline carbon nanotubes for hydrogen storage using molecular dynamics simulations**

**A THESIS**

*Submitted in partial fulfillment of the requirement for the award  
of the degree*

*Of*

**Master of Technology**

**In**

**Mechanical Engineering**

*With specialization in*

**Mechanical Systems Design**

*By*

**ANKIT KUMAR**



Discipline of Mechanical Engineering  
**Indian Institute of Technology Indore**

**DEC 2020**



# INDIAN INSTITUTE OF TECHNOLOGY INDORE

## CANDIDATE'S DECLARATION

I hereby certify that the work which is being presented in the thesis entitled **Polycrystalline carbon nanotubes for hydrogen storage using molecular dynamics simulations** in the partial fulfillment of the requirements for the award of the degree of **MASTER OF TECHNOLOGY** and submitted in the **DISCIPLINE OF MECHANICAL ENGINEERING, Indian Institute of Technology Indore**, is an authentic record of my own work carried out during the time period from DEC 2019 to DEC 2020 under the supervision of Dr. shailesh I. Kundalwal, Associate Professor, Dept. of Mechanical Engineering , IIT Indore.

The matter presented in this thesis has not been submitted by me for the award of any other degree of this or any other institute.

Ankit Kumar

-----

This is to certify that the above statement made by the candidate is correct to the best of my/our knowledge.

(DR. S. I. KUNDALWAL)

Signature of the supervisor of M.Tech. Thesis  
Dr. Shailesh I. Kundalwal  
IIT INDORE

-----  
Ankit kumar has successfully given his M.Tech. Oral Examination held on  
-----



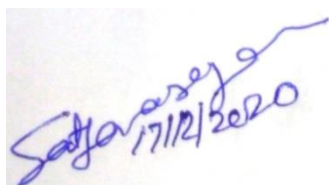
(DR. S. I. KUNDALWAL)

Signature of Supervisor of M.Tech. Thesis

Dr. Shailesh I. Kundalwal

Dept. of Mechanical Engineering

Date:



Signature of PSPC Member

Dr. Satyanarayan Patel

Dept. of Mechanical Engineering

Date:



Signature of PSPC Member

Dr. Lalit Borana

Dept. of civil Engineering

Date:



Signature of Convener, DPGC

Dr. Pavan K. Kankar

Dept. of Mechanical Engineering

Date: 18.12.2020

-----

## **ACKNOWLEDGMENT**

Firstly, I would like to express my deep sense of respect to Dr. Shailesh I. Kundalwal for providing me the opportunity to work under his supervision. I am very thankful to him for all his scientific discussions, immense knowledge and fruitful thoughts. His extreme energy, continuous encouragement, friendly interactions, and constructive support have enabled this work to achieve my goals. I highly appreciate for all his contributions which motivation for me to complete my research work comfortably.

I am extremely thankful to the Head of Department, Mechanical Engineering, IIT Indore for providing me all the facilities and their consistent support throughout the research work.

I am thankful to Mr. Nitin Luhadiya for their consistent support and his guidance and sharing their knowledge for this research work. I am also thankful to all the senior members and friends at ATOM Lab for their cooperation and their friendly nature.

Most valued, gratitude is expressed for my family members for their unconditional love, constant support and continuous faith on me and letting me be the chooser of my dreams and they also taught me to believe in myself at every situations.

Lastly, I would like to thanks to all my friends at IIT Indore, who made my life beautiful in IIT Campus and they also made my time enjoyable to a large extent at IIT Indore.

Ankit kumar



## ABSTRACT

Hydrogen storage and Adsorption hydrogen energy in both Pristine and Polycrystalline single-walled carbon nanotubes has been studied using molecular dynamics simulations (MDS). Research interest in hydrogen because of its pollution-free, abundance and high energy content in unit mass compare to other fuel. Hydrogen is an appropriate alternative in terms of green energy technologies for the carbon-based fossil fuels technologies. Hydrogen can be stored in solid adsorbent in terms of physisorption of hydrogen gas molecules in a safe and energy efficient manner.

The interaction between Carbon nanotubes (CNT) and hydrogen molecules, and interatomic interactions of the CNT are modeled via Lennard-Jones (LJ) potential using Tersoff potentials. Adsorption hydrogen energy and hydrogen gravimetric storage capacity are evaluated by the effects of various pressure and temperature using Potential energy distributions (PED). Adsorption hydrogen capacity are evaluated at different temperature i.e. 77 K, 100 K, 200 K, 273 K and up to 40 bar pressure starting from 1 bar for both Pristine and Polycrystalline single-walled carbon nanotubes. At 77 K and 20bar, the hydrogen gravimetric storage capacity of 6.2144% for pristine and 6.3133% for polycrystalline CNT and Adsorption hydrogen energy of -0.021ev for pristine and -0.0206ev for polycrystalline CNT is observed.

As the results obtained we observed that the decreasing in temperature and increasing in pressure, gravimetric density (GD) for hydrogen storage is increased for Pristine as well as Polycrystalline single-walled carbon nanotubes. Gravimetric density for hydrogen storage with the effect of grain boundaries in CNT i.e. Polycrystalline CNT is higher than Pristine CNT at different temperature and Pressure. The gravimetric density for hydrogen storage and adsorption hydrogen energy with the effect of different strain and defects is applied in both the Pristine CNT and polycrystalline CNT is evaluated.

# TABLE OF CONTENTS

ABSTRACT.....	5
LIST OF TABLES.....	v
LIST OF FIGURES.....	Error!
Bookmark not defined.	
ABBREVIATIONS.....	viii
<b>Chapter 1 Introduction.....</b>	<b>1</b>
1.1 Carbon Nanotube.....	1
1.2 Classification of Carbon nanotubes (CNTs).....	1
1.2.1 Single wall Carbon nanotubes (SWCNTs).....	2
1.2.2 Multi walled carbon nanotubes (MWCNTs).....	2
1.3 structure of carbon nanotube.....	3
1.4 Properties of Carbon Nanotubes.....	4
1.4.1 Mechanical Properties.....	4
1.4.2 Electrical Properties.....	5
1.4.3 Thermal Properties.....	5
1.4.4 Optical Properties.....	5
1.5 Grain boundary in carbon nanotubes .....	6
1.6 Voronoi tessellation.....	7
1.7 Energy overview.....	8
1.8 Hydrogen Storage Methods.....	10
1.8.1 Physical-based hydrogen storage.....	11
1.8.1.1 Liquid hydrogen.....	11
1.8.1.2 Compressed gas.....	12
1.8.1.3 Cold- and Cryo-compressed gas.....	12



1.8.2 Material- based hydrogen storage.....	13
1.8.2.1 Adsorbent hydrogen storage.....	13
1.8.2.2 Liquid organic hydrogen storage.....	13
1.8.2.3 Interstitial hydride hydrogen storage.....	13
1.8.2.4 Complex hydride hydrogen storage.....	14
1.8.2.5 Chemical hydrogen storage.....	14
<b>Chapter 2 Literature Review.....</b>	<b>15</b>
2.1 Literature Review.....	15
2.1.1 Hydrogen Storage in Single-Walled Carbon Nanotubes.....	15
2.1.2 Hydrogen Storage with the effect of strain and defect in Single-Walled Carbon Nanotubes.....	18
2.2. Research Gaps.....	20
2.3 Research objectives.....	20
<b>Chapter 3 Methodology.....</b>	<b>21</b>
3.1 Molecular dynamic simulation.....	21
3.2 Molecular dynamic integration algorithms.....	21
3.2.1 Velocity verlet algorithm.....	22
3.3 Design constraints of Molecular dynamic.....	23
3.3.1 Micro-canonical ensemble (NVE).....	23
3.3.2 Canonical ensemble (NVT).....	24
3.3.3 Isothermal-Isobaric (NPT) Ensemble.....	24
3.3.4 Generalized ensembles.....	24
3.4 Potential Fields.....	24
3.5 Equation of Motion.....	26
3.6 Methods of Controlling Pressure and Temperature.....	28

3.7 Process for hydrogen storage in carbon nanotubes.....	29
3.8 Adsorption isotherm equations.....	33
3.8.1 Langmuir Isotherm.....	33
3.8.2 Freundlich Isotherm.....	34
3.8.3 Sips (Langmuir–Freundlich) Isotherm.....	34
3.8.4 Fritz–Schlunder Isotherm.....	34
3.9 Modeling polycrystalline carbon nanotubes.....	34
3.10 Hydrogen storage considering strain.....	35
<b>Chapter 4 Results and discussion.....</b>	<b>37</b>
4.1 Hydrogen adsorption weight percent and hydrogen adsorption energy for pristine carbon nanotubes.....	39
4.2 Hydrogen adsorption weight percent and hydrogen adsorption energy for Polycrystalline carbon nanotubes.....	42
4.3 Hydrogen adsorption weight percent and hydrogen adsorption energy for pristine carbon nanotubes considering Strain.....	46
4.4 Hydrogen adsorption weight percent and hydrogen adsorption energy for defective carbon nanotubes.....	49
<b>Chapter 5 Conclusions.....</b>	<b>51</b>
<b>Reference.....</b>	<b>52</b>

## LIST OF TABLES

Table 3.1 Lennard-Jones interaction parameters for carbon atoms and hydrogen molecules.....	32
Table 4.1 Weight adsorption density of hydrogen molecules for pristine carbon nanotubes at different temperature at 20 bar pressure.....	40
Table 4.2 Weight adsorption density of hydrogen molecules for pristine and polycrystalline carbon nanotubes at 77K.....	45
Table 4.3 Weight adsorption density of hydrogen molecules for pristine carbon nanotubes at 77K and 20 bar Pressure.....	47

## LIST OF FIGURES

Figure 1.1 A carbon nanotubes.....	1
Figure 1.2 A Single wall carbon nanotubes (SWCNTs).....	2
Figure 1.3 A Multi wall carbon nanotubes (MWCNTs).....	3
Figure 1.4: Representation of chirality in sheet and carbon nanotube.....	4
Figure 1.5 Carbon nanotubes containing grain boundary.....	6
Figure 1.6 Voronoi diagram for obtaining grain boundary.....	7
Figure 1.7 Comprison btw world total primary energy consumption.....	8
Figure 1.8 Methods of production of hydrogen.....	9
Figure 1.9 Methods of hydrogen storage technologies.....	11
Figure 3.1 Change in position of an atom with time.....	23
Figure 3.2 Force-field degrees of freedom.....	25
Figure 3.3 Molecular dynamic simulation flow chart.....	26
Figure 3.4 System configuration of carbon nanotubes for hydrogen molecules.....	30
Figure 3.5 Formations of polycrystalline carbon nanotubes using graphene sheets.....	35
Figure 4.1 Simulation image for hydrogen storage in carbon nanotubes.....	37
Figure 4.2 Potential Energy Distribution (PED) of hydrogen molecules and front view and top view of the hydrogen molecules at 77 K and 1 MPa .....	38
Figure 4.3. Variation of hydrogen adsorption capacity (wt %) for pristine Carbon nanotube at constant pressure (20bar) (a) at different temperature (b) with different no. of steps (lakh) at 77k and 100 K.....	39

Figure 4.4 Variation of adsorption hydrogen wt% of Pristine carbon nanotubes with pressure at different temperature.....	40
Figure 4.5 Variation of adsorption hydrogen energy (eV) for Pristine carbon nanotubes with pressure at different temperature.....	41
Figure 4.6 Variation of adsorption hydrogen wt% for Polycrystalline CNTs with pressure at different temperature.....	42
Figure 4.7 Variation of adsorption hydrogen energy (ev) for Polycrystalline carbon nanotubes with pressure at different temperature.....	43
Figure 4.8 Hydrogen adsorption wt% comparison btw pristine and polycrystalline carbon nanotubes with different pressure at 77 K.....	44
Figure 4.9 Simulation image for hydrogen storage in CNTs Considering Strain.....	46
Figure 4.10 Variation of adsorption hydrogen wt% of Pristine CNTs considering Strain with strain at 20 bar pressure (a) at 77K (b) at 200K.....	47
Figure 4.11 Variation of adsorption hydrogen energy (eV) for Pristine CNTs considering Strain with different Strain at 20bar (a) at 200 K temperature (b) at 77K and 200K.....	48
Figure 4.12 Variation of (a) adsorption hydrogen wt% (b) hydrogen adsorption energy (ev) of polycrystalline carbon nanotubes with different strain at different temperature at 20 bar pressure.....	49
Figure 4.13 Comparison the hydrogen adsorption wt% at 20 bar pressure between (a) pristine CNTs and CNTs with Strain (6%) at different temperature (b) pristine and polycrystalline CNTs with different Strain at 200K temperature.....	50
Figure 4.14 Variation of hydrogen adsorption wt% for defective pristine carbon nanotube at different pressure at 77K and at different temperature.....	51
Figure 4.15 Variation of adsorption hydrogen energy (ev) for defective pristine carbon nanotubes with different pressure at different temperature.....	52

Figure 4.16 Variation of (a) adsorption hydrogen wt% (b) hydrogen adsorption energy (ev) of defective polycrystalline carbon nanotubes with different pressure at 77K and 100K temperature.....52

## LIST OF ABBREVIATIONS

CNTs	Carbon nanotubes
SWCNTs	Single walled carbon nanotubes
MWCNTs	Multi walled carbon nanotubes
PCNTs	Polycrystalline carbon nanotubes
MD	Molecular dynamics
PED	Potential energy distribution
LJ	Lennard- jones
MOF	Metal-organic frameworks
GD	Gravimetric density
VD	Volumetric density
PEM	Proton exchange membrane
DOE	Department of energy
GB	Grain boundary
LAMMPS	Large Scale Atomic/Molecular Massively Parallel Simulator
CTMD	Constant temperature molecular dynamics
REMD	Replica exchange molecular dynamics

**1.1 Carbon Nanotube**

Carbon nanotubes (CNT) are cylindrical hollow nanostructure molecules which is allotropes of carbon with diameters mainly measured in nanometers. Carbon nanotube mainly refer to single-wall carbon nanotubes (SWCNTs) which is independently discovered in 1993 by Iijima and Ichihashi [1] and Bethune et al.[2] in carbon arc chambers. Carbon nanotubes are formed by rolling of two-dimensional hexagonal lattice of graphene sheet to form a hollow cylinder.

Most of the researchers attract towards the carbon nanotubes due to highly attractive alternative to conventional composite materials because of their thermal, electrical, mechanical, barrier and chemical properties such as electrical conductivity, improved heat deflection temperature, increased tensile strength.

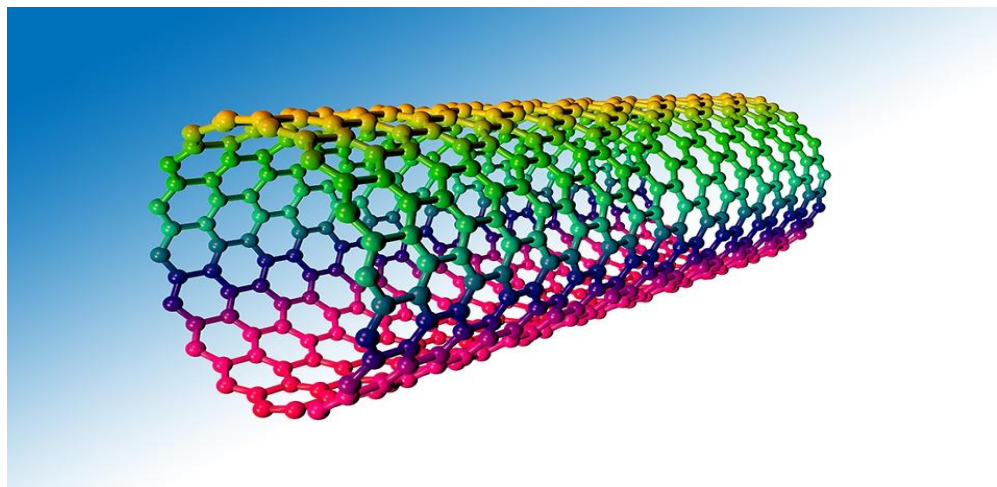


**Figure 1.1 A carbon nanotubes**

**1.2 Classification of Carbon nanotubes (CNTs)**

Carbon nanotubes are classified on the basis of the number of graphene layers present in carbon nanotube in two ways:

- Single walled carbon nanotubes (SWCNTs)
- Multi walled carbon nanotubes (MWCNTs)

### 1.2.1 Single wall Carbon nanotubes (SWCNTs)

Single wall Carbon nanotubes is formed by rolling single graphene sheet which is two-dimensional hexagonal lattice of carbon atoms and it is mostly found in rope-form with diameters in the range of a nanometer. The attention of researchers towards the SWCNTs because of their versatile nature of conductivity, high tensile strength due to  $Sp^2$  bond, flexibility, high effective surface area, hollow structure, light weight. And it is chemically bonded with  $Sp^2$  bonds which is extremely strong form of molecular interaction.

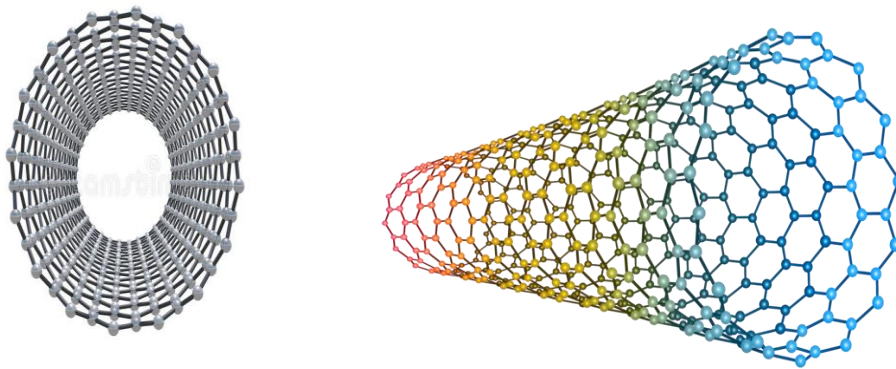


**Figure 1.2 A Single wall carbon nanotubes (SWCNTs)**

### 1.2.2 Multi walled carbon nanotubes (MWCNTs)

Multi wall Carbon nanotubes is formed by rolling multiple number of graphene sheets to form concentric hollow tubes cylinder. In MWNTs Carbon nanotubes are weakly bound together by van der Waals interaction which is tree ring-like structure. The interlayer distance between two nanotubes in multi-walled carbon nanotubes is approximately 3.4 Å. Multi wall Carbon nanotubes are similar morphology and properties as compare to single wall nanotube but they are more resistant to chemicals. Sometimes multi wall Carbon nanotubes are also known as double-wall and triple-wall carbon nanotubes.



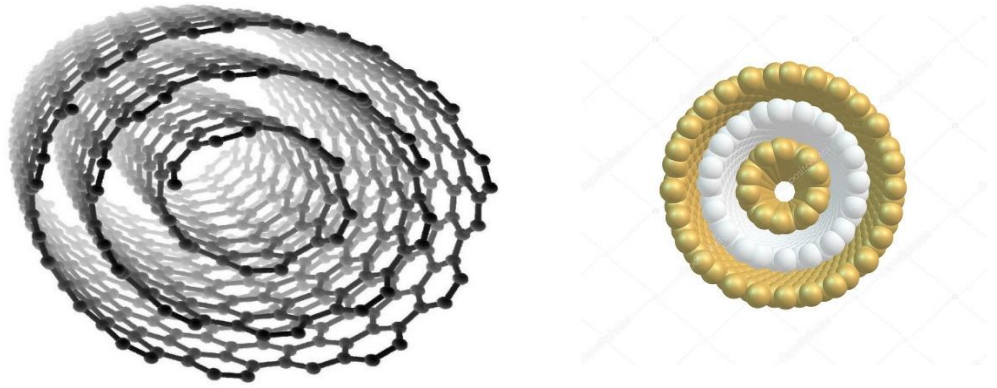


**Figure 1.3 A Multi wall carbon nanotubes (MWCNTs)**

### **1.3 structure of carbon nanotube**

The structure of a carbon nanotube is formed by a layer of carbon atoms that are bonded together in a hexagonal lattice and one-atom thick layer of carbon is referred as graphene and it is wrapped in the shape of a cylinder and bonded together to form a carbon nanotube. The structure of a carbon nanotubes are classified as armchair ( $n, m=n$ ), zigzag ( $n, m=0$ ) and chiral ( $n, m$ ) nanotube. Where  $n, m$  are the chiral index in  $x, y$  directions which is called index of vectors. Chiral vector [3] of nanotube is given by

$$\mathbf{C}_h = m \mathbf{a}_1 + n \mathbf{a}_2 \quad (1)$$

Here,  $n, m$  = chiral indices

And  $\mathbf{a}_1$  &  $\mathbf{a}_2$  are unit vectors of graphene sheet in the two-dimensional hexagonal lattice.

Diameter of carbon nanotube ( $D$ ) can be calculated from chiral indices is given by

$$D = \frac{\sqrt{3}a_{c-c}}{\pi} \sqrt{(n^2 + m^2 + nm)} \quad (2)$$

Where  $a_{c-c} = 1.42 \text{ \AA}$  is the equilibrium bond length of graphene

$D$  is the diameter of carbon nanotube

And  $m$  and  $n$  are the chiral indices.

On the basis of chiral indices different types of a carbon nanotube is defined as,

- If chiral indices i.e.  $\mathbf{m} = \mathbf{0}$  than it is known as zigzag carbon nanotubes and its chiral angle is equal to  $0^\circ$ .
- If chiral indices i.e.  $\mathbf{n} = \mathbf{m}$  than it is known as armchair nanotubes and its chiral angle equal to  $30^\circ$ .
- If chiral indices i.e.  $\mathbf{n} \neq \mathbf{m}$  than it is known as chiral nanotubes and its chiral angles lie between  $0$  and  $30^\circ$ .

The two-dimensional structural of carbon nanotube as shown in figure 1.4 shows the two-dimensional graphene sheet with chiral indices  $(n, m)$  where mainly  $n \geq m$  [4].

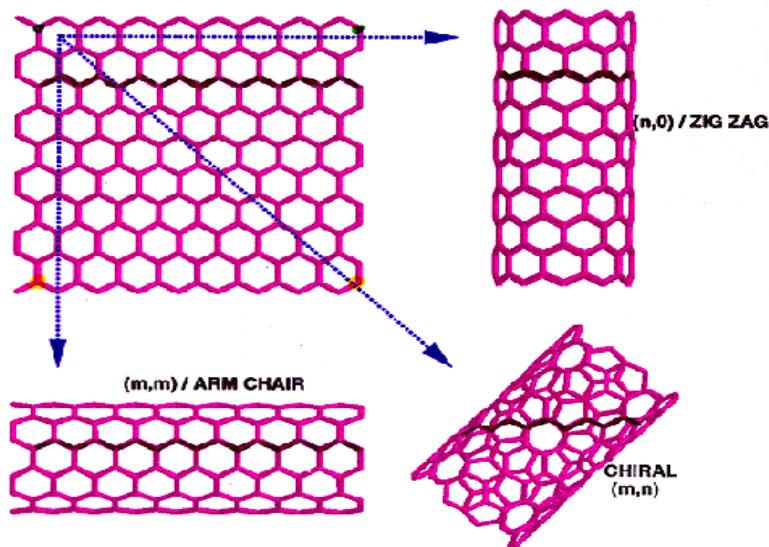


**Figure 1.4 Representation of chirality in sheet and carbon nanotube**

## 1.4 Properties of Carbon Nanotubes

### 1.4.1 Mechanical Properties

Carbon nanotubes are the strongest and stiffest materials in terms of tensile strength and elastic modulus. Covalent  $\text{Sp}^2$  bonds formed between the individual carbon atoms which gives more strength. Strength of individual carbon nanotubes shells is very high, weak shear interactions between adjacent shells and tubes but the effective strength of multi walled carbon nanotubes is reduced by a few GPa. Due to high mechanical toughness of carbon nanotubes

is important in their application as mechanical elements such as robust atomic force microscopy and for high aspect ratio structures [5]. Carbon nanotubes are very soft in the radial direction due to Young's modulus in the order of various GPa.

#### **1.4.2 Electrical Properties**

Carbon nanotubes have high electrical conductivity in plastics and their high aspect ratio i.e.1000:1 imparts high electrical conductivity due to highly conducting it is said to be metallic. Their conductivity is shown to be a function of the degree of twist, diameter and their chirality. The conductivity and resistivity has been measured by the placing electrodes at different parts of the CNTs for the ropes of single walled Carbon nanotubes. So, we say that single walled Carbon nanotube ropes are the most conductive carbon fibers.

#### **1.4.3 Thermal Properties**

Thermal property of the material is defined for the behavior of any material when it is subjected to a change in temperature or heat. Structural changes and temperature increases in Carbon nanotubes due to heat is applied and it is absorbed and transported within the material. When the heat is applied continuous it may even result in melting and carbon nanotubes show high thermal Conductivity and low thermal Expansion Coefficient.

Thermal conductivity is defined as the ability of the material to transfer heat from high temperature to low temperature. The expression is given by,

$$q = -k \frac{dT}{dx} \quad (3)$$

where q is the heat flux per unit time per unit area

And k is the thermal conductivity,

And  $dT/dx$  is the temperature gradient through the materials [6].

#### **1.4.4 Optical Properties**

The optical properties of carbon nanotubes are highly relevant for the materials science and these materials are interact with electromagnetic radiation is unique and it is useful for the peculiar absorption, photoluminescence (fluorescence), and Raman spectroscopy. Spectroscopic

methods is used for the quick and non-destructive characterization of adequately large amounts of carbon nanotubes. And it is also potentially useful in the aforementioned tunability of properties which is optics and photonics. Light-emitting diodes (LEDs) and photo-detectors based on a single carbon nanotube have been developed in the lab.

### 1.5 Grain boundary in carbon nanotubes

Carbon nanotubes which is synthesized from chemical vapor deposition is defined as polycrystalline and contain one-dimensional defects i.e. grain boundaries(GB).It is line of individual point defects which is generally tilted boundaries. [7] Grain boundary is a two-dimensional defect which is the interface between adjacent grains or the boundary between crystals of a defects material.

In many study it is found that the effect of the grain boundary is minimum as compared to other materials in carbon nanotubes. From here we observed that the electrical performances of the device was not significant due to the the effect of grain boundaries and due to this it does not degrades the electrical performance. Now due to the grain boundaries also, it was found that adsorption capacity of carbon nanotubes is increases [8]. So we can observed that the carbon nanotubes with grain boundaries i.e. polycrystalline carbon nanotubes becomes important.

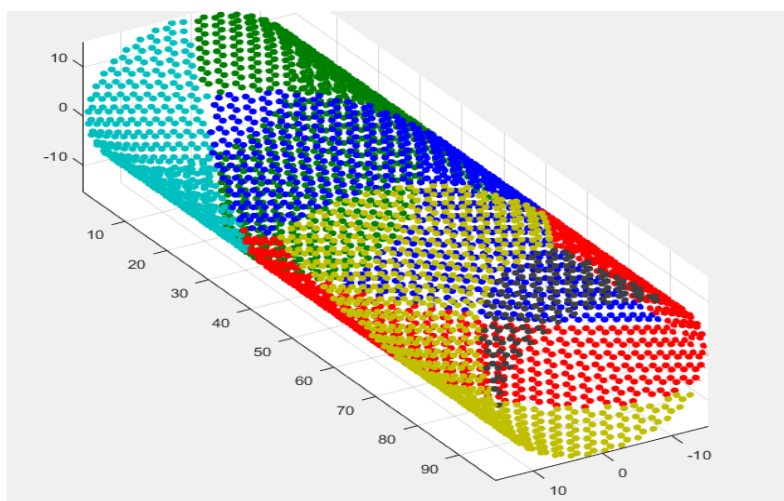


**Figure 1.5 Carbon nanotubes containing grain boundary**

Many studies stated that the intrinsic strength, failure mechanism of carbon nanotubes and critical failure strain with grain boundaries mainly depends on the temperature and dihedral angle. Due to the grainy structure in carbon nanotubes the mechanical properties of polycrystalline solids are strongly influenced and carbon nanotubes have produced in a controlled environment and these are less susceptible to large extrinsic defects. Due to this it is expected that the variations in their mechanical properties to emerge from intrinsic grain boundaries. Crack initiation within the carbon nanotubes is introduced because stress state is introduced due to grain boundary. So due to lack of inclusive understanding for the influence of grain boundaries which may restraint the exploitation of the properties of polycrystalline carbon nanotubes.

### **1.6 Voronoi tessellation**

Voronoi diagram is a division of a plane into regions near to the given set of objects and it is mainly studied in mathematics. Voronoi diagram is obtained by joining the set of all points in the plane that are nearer to each site than to other sites which is finitely many points in the plane. Corresponding region for each seed consist of all points of the plane near to that seed compare to other seeds. Voronoi diagram is obtained by joining the set of all points as shown in Figure 1.6.

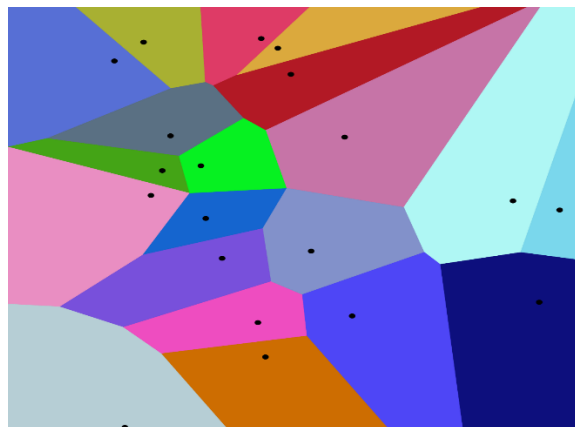


**Figure 1.6 Voronoi diagram for obtaining grain boundary**

Voronoi tessellation is a method which is used for creating grain boundaries and the main thing is that we select any point to the region in which to join all the point is nearer to that particular point to form the voronoi diagram. Voronoi tessellation is mainly used to identifying the nearest shop, risk calculation of virus infection, computer science, etc. In our study Voronoi tessellation is used for creating the grain boundary in pristine carbon nanotubes containing some crystals i.e. grain size to convert into polycrystalline carbon nanotubes i.e. carbon nanotubes with grain boundary.

### 1.7 Energy overview

Current scenario of energy which is dependence on non-renewable sources of energy i.e. carbon-based fossil fuels. But due to more consumption of carbon-based fossil fuels it caused various environmental pollution and depletion of the fossil fuel as shown in Figure. 1.7. So we can find an alternative of carbon-based fossil fuels which can reduce the pollution and depletion of fossil fuels and by replacement of fossil fuel we can save the world from energy crisis and severe global warming. Due to continuous growing demand of energy and severe global environmental concerns, many research has been done to find an alternative source of carbon-based fossil fuels.

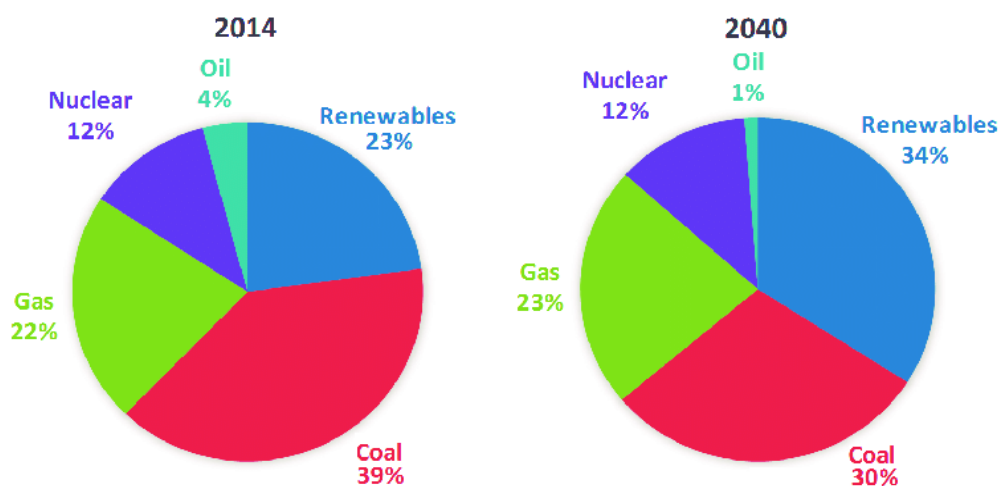


**Figure 1.7 Comprision btw world total primary energy consumption**

So we can use renewable sources energy including solar energy, wind energy, hydropower, biomass energy etc. have received a more attention on these energy. Among all these energy hydrogen has been believed an important and promising energy and research interest in hydrogen because of its pollution-free, abundance and high energy content in unit mass compare to other fuel. Hydrogen is an appropriate alternative in terms of green energy technologies for the carbon-based fossil fuels technologies. But the hydrogen storage as efficiently and safely is still a challenge to recognize its economy. Therefore hydrogen is a significantly available source of energy and hydrogen is present in the form of water and forming several other compound with component like, carbon, nitrogen etc. So we can used to produce the hydrogen gas to use as a fuel as renewable sources energy. Recently hydrogen has been produced from various renewable resources such as biomass, solar, wind. There is a method for hydrogen production by using the splitting of water using electrolysis or using solar energy or from several biological processes by environment-friendly ways as shown in Figure. 1.8. Biomass gasifications and electrolysis process using wind found to be cost-effective technology and the expectation is the commercialization by solar electrolysis process.

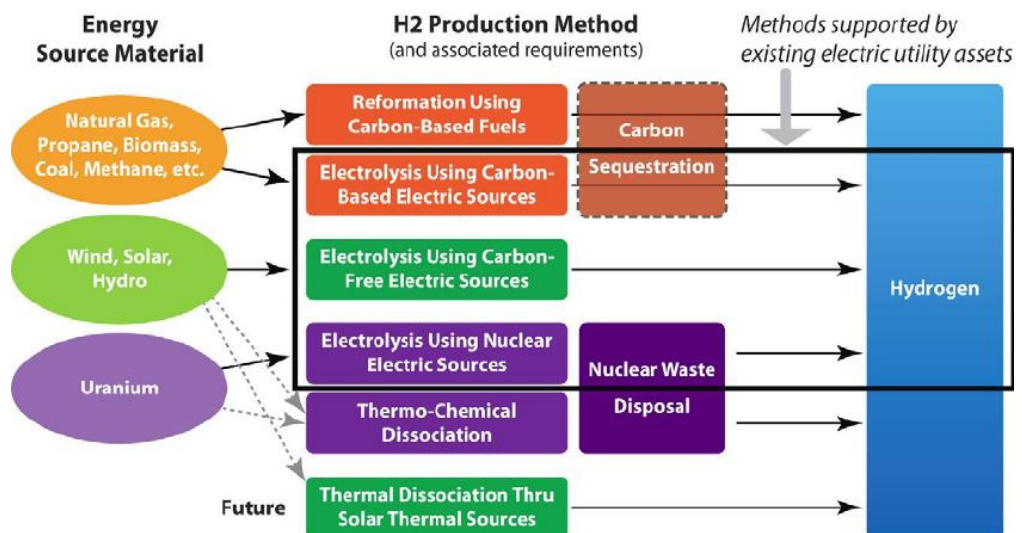


**Figure 1.8 Methods of production of hydrogen**

Application of hydrogen fuel is widespread which is especially used in the automobile industry and it is prevented by the efficient on-board storage and

lack of safe and release systems and the major concern of fuel as hydrogen is storage and utilization in our daily life. Hydrogen storage in terms of gravimetric density, based on mass and volumetric density (VD), based on volume in which the target set by U.S Department of Energy (DOE) as the standardizing of the hydrogen storage. Vehicles which is powered by hydrogen can produce zero emissions and it cannot leave any carbon footprint on the environment as compare to the conventional fossil fuels.

Hydrogen as a green source of energy which can developed the proton exchange membrane (PEM) fuel cells and it can happen because of the exploring major driving forces. The main problem is to how the hydrogen is storage in the efficient on board storage and release of hydrogen. The path is developed for the hydrogen storage from hydrogen production to hydrogen vehicle in terms of on board storage as shown in fig 1.9. Hydrogen may be stored in an empty tank or in a tank which contains a solid which is solid based storage by using on board storage. Gravimetric storage density is determined by considering only the weight of solid in solid storage which is compare with the material's performance for the vessel-based storage [9].

## **1.8 Hydrogen Storage Methods**

Hydrogen is an amply available source of energy which is the most suitable candidate for the alternative energy sources due to its high energy content per unit mass, utilization efficiency, and environmental compatibility [10, 11,12]. Proton exchange membrane fuel cells is the most promising uses for hydrogen for power generation in vehicles [13, 14]. Storage of hydrogen in a compact, light, and cost efficient manner is a technical challenges in a vehicle is the bottleneck intercept its wide-spread for the use of the energy carrier [15, 16, 17]. Electrochemical devices fuel cell is mainly used for providing power for the vehicles in which hydrogen and oxygen combined together to produce electricity and hydrogen converts into electricity about 50% efficiency and it can produces heat and water as a by-product.



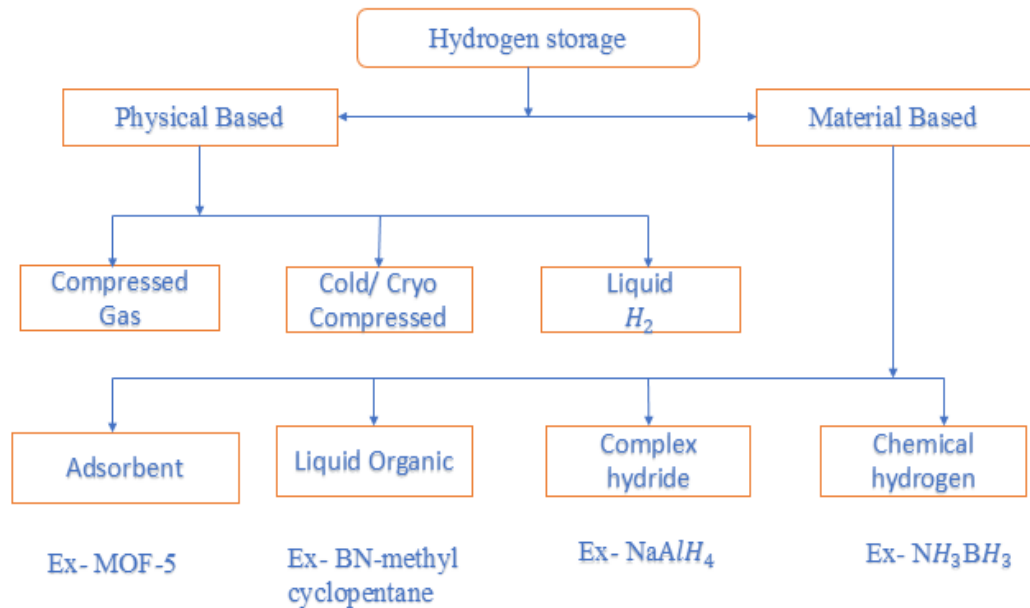


**Figure 1.9 Methods of hydrogen storage technologies**

Hydrogen storage methods is defined mainly in two different ways:

- ❖ Physical-based hydrogen storage
- ❖ Material-based hydrogen storage

#### 1.8.1 Physical-based hydrogen storage

Physical-based hydrogen storage in a vessel is defined in terms of:

- Liquid hydrogen
- Compressed gas
- Cold / Cryo compressed

##### 1.8.1.1 Liquid hydrogen

At specific Pressure and temperature so that storing hydrogen is get liquefied by using liquid hydrogen storage method and it requires a high level of purity. Hydrogen should be cooled below the critical temperature of 33 K, since it is economically but not efficient because it will require very large setup and plant and this hydrogen storage process is complex. Therefore liquid hydrogen storage is difficult and evaporation can take place and its application is finite used in space travel.

#### 1.8.1.2 Compressed gas

Compressed hydrogen is a storage form in which hydrogen gas is kept under the pressures range of 350 bar to 700bar to increase the storage density and hydrogen is stored as the gas inside the cylinders and in tanks. Compressed gas hydrogen method is not good because of its cost efficiency and energy efficiency due to this it is not considered commercially. Hydrogen which is compressed form is stored in tanks which is made of polymer and composite material at very high pressure and it can be supported by the mechanical forces. Compressed hydrogen is used for the hydrogen tank systems in vehicles and automobiles industry and it is based on carbon-composite technology because fueling of hydrogen gas is very rapid [18]. Transportation of compressed gas is easy by trucks in gas cylinders or gas pipelines in which pressures is ranging from 200 to 500 bar. Hydrogen density of compressed gas is about  $20 \text{ kg/m}^3$  is reached at 300 bars and high-pressure gas steel cylinders is operated at maximum pressure of 200 bar which is common type of storage system.

#### 1.8.1.3 Cold- and cryo-compressed gas

Cold- and Cryo-compressed hydrogen storage methods refers to the storage of hydrogen at cryogenic temperatures in a vessel and it can be pressurized for the pressure range of 250 bar to 350 bar but in contrast to current cryogenic vessels in which liquid hydrogen can store at near-ambient pressures. Cryo- compressed is similar to liquefied hydrogen where hydrogen is compressed at temperature 20K approximately and it gives higher energy density with a slight modification. The difference between Cold- and Cryo-compressed hydrogen and liquid hydrogen storage is, if the hydrogen gets heat up with the heat transfer from the environment than there is a system which can allows us to go to higher pressure and they provide us to get enough hydrogen for the utilization in the vehicle.

### 1.8.2 Material- based hydrogen storage

Material- based hydrogen storage methods is classified into different categories where hydrogen is adsorbed on the surface and it is classified as,

- Adsorbent
- Liquid organic
- Interstitial hydride
- Complex hydride
- Chemical hydrogen

#### 1.8.2.1 Adsorbent hydrogen storage

Adsorbent hydrogen storage in which adsorbent materials can allow a liquid, gas, and dissolved solid to bond a materials to it's a surface. Hydrogen can adsorbed by the chemisorption and the physisorption process of hydrogen on high surface area materials, such as Metal-organic frameworks (MOFs). Adsorption of hydrogen gas on solid is a safe, less expensive and energy efficient method compared to other methods and it also have a potential to reach the DOE goal and at a certain desorption pressure physisorbed hydrogen can be desorbed by decreasing the pressure.

#### 1.8.2.2 Liquid organic hydrogen storage

The storage of hydrogen in liquid organic hydrogen storage systems have safe and efficient method over conventional storage systems. Liquid organic can give a flexible medium for hydrogen storage and transportation of renewable energy in the form of the existing fuel such as B-N methyl cyclopentane. Hydrogen storage liquid organic systems requires an exothermic hydrogenation step and an endothermic dehydrogenation step from a thermodynamic point of view and hydrogenation and dehydrogenation can be take place at the same temperature level.

#### 1.8.2.3 Interstitial hydride hydrogen storage

Hydride materials have good energy density and their specific energy is worse than the leading hydrocarbon fuels. Liquids fuels at ambient temperature and pressure are easy to fuel but others are solids which could be convert into pellets. It can forms the compound with the metals in the interstitial hydride hydrogen storage and compound are such as  $\text{LaNi}_5\text{H}_6$ . Hydrogen storage in

terms of interstitial-hydrides are also fails for most of the materials with respect to the total weight of the storage system.

#### 1.8.2.4 Complex hydride hydrogen storage

Complex hydrides are potential candidates for materials based hydrogen storage because of their high gravimetric hydrogen density. Complex hydrides are very important and promising materials for hydrogen storage applications, material such as Sodium aluminium hydride i.e.  $\text{NaAlH}_4$ . Complex hydrides are metal salts which contains more than one metal or metalloid in which the anion contains the hydride and it also contain transition metal hydrogen complexes in their structure and it has high volumetric densities.

#### 1.8.2.5 Chemical hydrogen storage

Chemical hydrogen storage can give high energy densities and it is potential use of the systems involve liquids that may be easily dispensed using infrastructure for the gasoline refueling stations. It also work under the process of electrochemical hydrogen storage system. Chemical compounds with hydrogen can also be considered as a hydrogen storage and it includes such as methanol, ammonia, and methyl cyclohexane and compound like Ammonia borane i.e.  $\text{NH}_3\text{BH}_3$ .

**2.1 Literature Review****2.1.1 Hydrogen Storage in Single-Walled Carbon Nanotubes**

Carbon Nanotube(CNT) have attracted a lot of researchers' attention due to their high specific surface area (SSA) and pore sizes in nanometer range and show great potential to adsorb hydrogen in their nano-structures[19][20]. Hydrogen is promising energy for the hydrogen adsorption in Carbon nanotube and growing research interest in hydrogen because of its abundance, pollution-free and packing more energy per unit mass compare to other fuel [21]. Hydrogen storage system should be safe, portable, compact, cost-efficient, and speed of kinetics which is the speed of stopping when it required and the rate of release of hydrogen on demand [22]. Hydrogen storage can be defined in two methods i.e. one is physical storage based on cryogenic temperatures and utilizing high pressures and second one is material storage based on physisorption and chemisorption [23].

Physisorption principles is the hydrogen adsorption performance of a porous solid is maximized when a few molecular diameters is larger than that of pores [24]. Physisorption produce weak van der Waals forces of attractions because the presence of fluctuating dipole moments on the interacting adsorbate and adsorbent and produced a stronger interaction force due to the potential fields produced at the wall overlap which occurs in adsorption on a simple plane. Material based hydrogen storage i.e. physisorption is an attractive method as hydrogen does not chemically react to the substrate and it does not contaminate the fuel for transportation purposes [25].

Chemisorption process i.e. material based hydrogen storage to be reversible upon heating of the functionalized carbon nanotubes and then suggesting an important path for the development of CNT based hydrogen storage devices. And the formation of a strong C-H chemical bond at the carbon nanotube sidewall potentially diminish the reversibility of the hydrogen adsorption process for CNT, and practicability of chemisorption is used in real applications[26,27]. And there is no chemical dissociation of molecules to

provide faster kinetics for refueling and discharging as incompatible to reactive hydrogen storage [28].

Many authors have extensively studied the experimentally and computationally for hydrogen storage in Carbon nanotubes (CNT) and Carbon nanofibers (CNF) [29, 30, 31, 32, 33]. Carbon nanotubes have higher heat of adsorption than graphene and activated carbon due to the unique curvature effect which is determined by the tube diameter [34, 35]. By these features it make more suitable candidate for hydrogen storage than graphene. Many studies on carbon nanotubes exist by optimizing specific parameters such as temperature, pressure, inter-tube spacing, tube diameter, etc., to achieve higher hydrogen adsorption [36, 77, 38].

For carbon nanotubes, at very low tube diameter ( $<5 \text{ \AA}$ ), nanotube has been fractured after hydrogen storage. Between the tube diameter ranges from  $5 \text{ \AA}$  to  $12 \text{ \AA}$ , SWCNT's wall has been strained after hydrogen storage and Large tube diameter ( $>21 \text{ \AA}$ ), SWCNT's has been self-collapsed at the time of release of hydrogen adsorption. In between the tube Diameter ranges from  $13 \text{ \AA}$  to  $20 \text{ \AA}$ , SWCNT's has obtained optimum hydrogen adsorption without ruptured [39].

Darkrim and Levesque et al. [40] state that as the diameter increases of carbon nanotube, the number of hydrogen to be entered inside the carbon nanotube is also increases for hydrogen storage. For the monolayer hydrogen adsorption take place for the tube diameter above  $10 \text{ \AA}$  bulk density can be reached out inside the nanotube also at room temperature.

B. Kurniawan and N. Nasruddin et al. [41] obtained optimum hydrogen storage in carbon nanotube in between the tube diameter range of  $8\text{-}10 \text{ \AA}$  and it also found very less amount of hydrogen adsorption in carbon nanotube approximately 1-2 wt% at ambient temperature. Therefore it is needed to be manipulated to make it suitable for the ambient hydrogen adsorption for nanotube structure.

Cracknell et al. [42] state that, because of their curvature effect the hydrogen adsorption of carbon nanotubes is relatively higher inside the nanotube comparatively than outside the nanotube. Gravimetric storage capacity of carbon nanotube has been obtained above the DOE target (approximately 8wt %) in literature at temperature approximately 80 K and at the maximum pressure of approximately 150atm [43, 44].

Thermal motion of hydrogen molecule increases in carbon nanotube with increases in temperature, so at room temperature hydrogen storage capacity is considerably decreases [45]. So, at this temperature, the efficiency of SWCNT decreases due to increase in kinetic energy of hydrogen molecules and it becomes very less hydrogen adsorption in one single wall carbon nanotubes [46] and the less thermal motion and potential energy dominating nature of hydrogen molecules at low temperature (approximately 80K) due to this van der Waals interactions become very effective which lead to more hydrogen adsorption in one single-walled carbon nanotube [47].

Juarez-Mosqueda et al. [48] stated that carbon nanotube ( $d_{\text{max}}$ : 13.56 Å) can chemisorb and desorb hydrogen molecules only by taken a significant energy barrier and they can absorb hydrogen molecules in carbon nanotube for a long time at very high gravimetric/volumetric density. They have also established the platinum (Pt) nanoparticles are very versatile on the  $Sp^2$  hybridization of carbon in carbon nanotube and then relocate nearly energy barrier-free.

Transition metals is presence in carbon nanotube then it decreases the hydrogen gravimetric storage density because of the heavy atomic mass of the metals is present. But light weight lithium can be doped in carbon nanotube can increase the gravimetric hydrogen storage density up to approximately 14 wt. % [49]. Rangel et al. [50] obtained hydrogen storage density of about 2.7 wt% at room temperature using lithium doped in carbon nanotube which is near about the experimental value [51, 52].

Ghosh and Padmanabhan et al. [53] states that the hydrogen storage density of Titanium and beryllium (Be) is doped in carbon nanotubes (CNTs) which contains Stone-Wales defects was studied using MDS and DFT. And Be-doped carbon nanotubes showed a promising potential to absorb hydrogen in CNTs exceed the above US DOE goal at room temperatures and high pressures.

Kundalwal et al. [54] studied the mechanical properties and the fracture behavior of large diameter polycrystalline CNTs (orientations of the grain boundary) of structure orientation, varied size, and structure to an applied in uniaxial load using MDS. And this is the first study in the literature which described the mechanical properties of polycrystalline carbon nanotubes.

### **2.1.2 Hydrogen Storage with the effect of strain and defect in Single-Walled Carbon Nanotubes**

Xue and Xu et al. [55] states that the binding energies, atomic structures, electronic and mechanical properties of graphene are considerably modified by applying strain and about 10% of biaxial strain, binding energies of hydrogen on graphene can be enhanced by 53.89% and 23.56% in the symmetric and antisymmetric phase using the first-principle of calculations.

Shikai deng et al. [56] states that the strain can modifies the thermal conductivity, atomic structure, chemical activity, lattice vibration, and mechanical properties in 2D nanomaterials. And the chemically inert monolayer graphene becomes effective by strain engineering using the first principle study [57].

Zhou and Lu et al. [58] study about the use of mechanical strain as signify to sustain metal atoms on carbon-based substrate and to increase the hydrogen adsorption. And also studied the strain effects on hydrogen storage capacity of metal-decorated graphene and we see that tensile strain in graphene can sustain the supported metal atoms, and increase the hydrogen adsorption. Hydrogen



storage capacity obtained up to 15.4 wt. % on Li- decorated and 9.5 wt. % on Ti-decorated graphene with a strain of 10% and about 0.2 eV/H<sub>2</sub> can obtained the optimal binding energy.

Li- decorated the lightest alkali metal and Ti- decorated a commonly used as light transition metal, are used as model systems for two-dimensional (2D) graphene sheets [59]. Over 15% of strain can be easily implement in graphene as demonstrated the experimentally, [60, 61] which is important for optical and electronic applications. [62, 63] The tensile strain around 10% could extremely increase the hydrogen adsorption and there is catalytic activity of metal clusters on graphene [64].

Defects obtained in carbon nanostructure and carbon nanotube have been theoretically described by Stone and Wales in 1986 is known as called Stone-Wales defects [65]. At a high range of temperature mono-vacancy or di-vacancy can be formed in single wall carbon nanotube and grapheme, it is formed as 5, 8, 9 -membered rings [66].

Gayathri and Geetha et al. [67] study about to calculated the adsorption energies in defective CNTs for distinct hydrogen configurations and obtained that the binding energy increased considerably when defects in CNTs were introduced and their study also says that hydrogen storage density could be increased for defective carbon nanotubes.

Chen et al. [68, 69] state that the experimental study in the presence of defects, mainly in micro-sizes (<20 Å) for carbon nanotubes surface increased the hydrogen adsorption at high temperature and at low temperature in 2008 and 2009 respectively due to this, the effect of nature of defects are still unknown. So, it becomes highly important to completely understand the mechanics of hydrogen storage capacity on carbon nanotubes considering structural defects.

## 2.2. Research Gaps

- Many authors have investigation of well-known defects such as atom vacancies, doping, substitutional impurities, Stone–Wales, and hybridization in smaller diameter carbon nanotubes. But There is no any authors is study about the application of PCNTs (considering Grainboundary ) and large diameter CNTs for hydrogen storage considering the effect of pressure and Temperature, for larger CNT diameter and PCNTs (considering Grainboundary) hydrogen storage is more.
- There is very few studies for hydrogen storage in carbon nanotubes bundles, CNTs bundles have high surface energy and surface area, Therefore, the application of CNT as well as PCNT bundles for hydrogen storage should be considered because it is more practical and realistic representation of their existence in bulk form to achieve the recent storage target set by the US DOE (8-10%).
- With considering the effect of pressure and Temperature, no single MDS study to investigate the hydrogen storage capacity and hydrogen adsorption energy for both Pristine CNTs and Polycrystalline carbon nanotube (PCNTs).

## 2.3 Research objectives

- Calculate the hydrogen adsorption capacity of pristine carbon nanotube (CNT) with considering the effect of pressure and Temperature.
- Creating grain boundary in CNTs and calculate the hydrogen storage capacity of Polycrystalline carbon nanotube (CNT with grain boundary) with considering the effect of Pressure and Temperature.
- Determine the hydrogen adsorption energy for both Pristine Carbon nanotube (CNT) and Polycrystalline carbon nanotube with considering the effect of Pressure and temperature.
- Consider the effect of strain and defects in carbon nanotube and obtain the hydrogen adsorption capacity and adsorption energy of defective carbon nanotube.

**3.1 Molecular dynamic simulation**

Molecular dynamics (MD) is a computer simulation method for investigating the physical movements of atoms and molecules. Molecular dynamic simulation allow us to study the mechanisms and behaviors of nanomaterials that no other simulation method can execute in a computationally efficient manner. It is dependent on time the computer simulations at molecular level allow us to find a new observation which is difficult to find in experimental way. Molecular dynamics simulations can also be used to verify any theory with experimental results. With the use of computer simulations, we can easily find out the reason of the phenomena by studying it in molecular level. MDS is study using the Large Scale Atomic/Molecular Massively Parallel Simulator (LAMMPS), an open-source package developed by Sandia National laboratories [70]. Molecular dynamics is the most comprehensive molecular simulation method which determine the motions of individual molecules. Molecular dynamics is a mechanics-based computer simulation method in which the time evolution of a set of interacting atoms is followed by integrating their equations of motion.

**3.2 Molecular dynamic integration algorithms**

Integration Algorithms is study about the initial position of atomic which is a function of the potential energy of all the atoms in the system in molecular dynamics simulation. The equations of motion must be solved numerically because nature of this function is quite difficult and it is not possible to solve by analytically.

Several numerical algorithms method is applied in molecular dynamics simulation to solve the equations for integrating such as Predictor-Corrector algorithm, Gear Predictor-Corrector algorithm, leap-frog algorithm and velocity verlet algorithm [71] but in our study velocity varlet algorithm is efficient method for integrating the equations of motion.

General Rules for integration algorithms in molecular dynamics simulation such as energy should be conserved and reversible, computational efficient, required long integration time step and required only one force evaluation per time step, it should be fast and require little computer memory, for the correct statistical ensembles energy should be conserved.

### 3.2.1 Velocity verlet algorithm

Velocity Verlet Algorithm is allowed to integration of newton's equation of motion to find positions ( $r(t)$ ), velocities ( $v(t)$ ), and accelerations ( $a(t)$ ), of the atom at time  $t$  are given by the three-dimensional vectors in one-time step, atoms are allowed to move and accelerate. Finding the new position of an atom which is determined by using Velocity Verlet Algorithm by integrating the equation of motion which is shown below.

$$\mathbf{v}\left(\mathbf{t}_0 + \frac{\Delta t}{2}\right) = \mathbf{v}(\mathbf{t}_0) + \mathbf{a}(\mathbf{t}_0) \frac{\Delta t}{2} \quad (4)$$

$$\mathbf{r}\left(\mathbf{t}_0 + \frac{\Delta t}{2}\right) = \mathbf{r}(\mathbf{t}_0) + \mathbf{v}\left(\mathbf{t}_0 + \frac{\Delta t}{2}\right) \Delta t \quad (5)$$

$$\mathbf{v}\left(\mathbf{t}_0 + \frac{\Delta t}{2}\right) = \mathbf{v}\left(\mathbf{t}_0 + \frac{\Delta t}{2}\right) + \mathbf{a}(\mathbf{t}_0) \Delta t \quad (6)$$

Where,

$r$  = position of the atom,

$v$  = Velocity of the atom,

$a$  = acceleration of the atom.

$t_0$  = initial time and  $\Delta t$  = time step.

Change in position, velocity, accelerations of an atom and time step with respect to time is shown in figure 3.1.

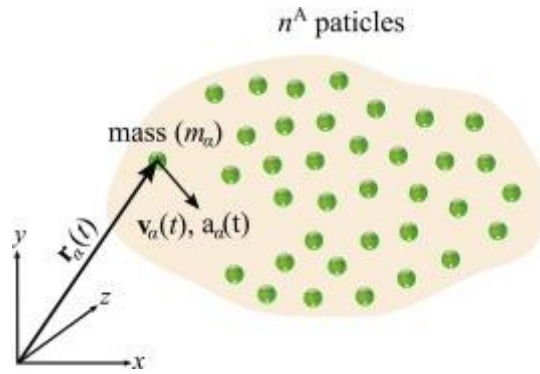


**Figure 3.1: Change in position of an atom with time**

Molecular dynamics simulations are implemented in constant pressure and constant temperature which is obtained by controlling the velocity and size of the simulation box and it is necessary to control the pressure and temperature in a natural environment for the system.

For controlling these properties several methods are used which are discussed below.

### **3.3 Design constraints of Molecular dynamic**

Molecular dynamics simulation should be designed by taking the account for the available computational power. Time step, total time duration and simulation size ( $n$  = number of particles) must be selected so that the calculation can be completed within a reasonable time period. However, external pressure and heat transfer is exposed to the environment for the most natural phenomena of the system. For these conditions, the total energy of the system is not conserved for long time and then we required the extended forms of molecular dynamics.

#### **3.3.1 Micro-canonical ensemble (NVE)**

Micro-canonical ensemble (NVE) in which changes in moles ( $N$ ), volume ( $V$ ) of the system, and energy ( $E$ ) of the system is isolated from system [72] and it is obtained by solving the Newton equation of motion. NVE is also corresponds to an adiabatic process with no heat exchange. Therefore, total energy being conserved but during the integration process there is a slight variation or float in energy due to rounding and truncation errors.

### **3.3.2 Canonical ensemble (NVT)**

The amount of substance (N), volume (V) of the system and temperature (T) are conserved in the system [72] and it is also referred as constant temperature molecular dynamics (CTMD) and it is obtained by controlling the temperature of the system. Using thermostat the energy of exothermic and endothermic processes is exchanged and also to add and remove energy from the boundaries of an MD simulation. In Canonical ensemble, the models of simulation is suitable in a vacuum without periodic boundary conditions.

### **3.3.3 Isothermal-Isobaric (NPT) Ensemble**

The amount of substance (N), pressure (P) of the system and temperature (T) are conserved in the system [72] and it is also referred as constant pressure and temperature ensemble and it is also useful for measuring the equation of state of model systems. Isothermal-Isobaric (NPT) Ensemble of select when the correct pressure, volume, and densities are important in the simulation of the system and the simulation is carried out in equilibrium to achieve the desired temperature and pressure and for using a thermostat we need a barostat.

### **3.3.4 Generalized ensembles**

Generalized ensemble is mainly the exchange method of model simulation and it was originally designed to deal with the slow dynamics of disordered spin systems and it is also referred as parallel tempering. Replica exchange molecular dynamics (REMD) have tries to exchange the temperature of non-interacting model of the system running at various temperatures to overcome the multiple-minima problem.

## **3.4 Potential Fields**

A molecular dynamics simulation requires the definition of a potential fields for the interatomic interaction of the carbon atoms in carbon nanotubes was modeled by using Tersoff potential and this potential field is the mathematical expression of the potential energy of atoms [73]. Potential fields are empirical in nature in which parameters are mainly obtain from experimental methods

and high-level quantum mechanics approaches. Force fields is the pair potential i.e. total potential energy which is calculated from the sum of energy contributions between pairs of atoms. Potential fields of an atom is defined below

$$E_{\text{total}} = E_{\text{covalent}} + E_{\text{non covalent}} \quad (7)$$

Where  $E_{\text{total}}$ ,  $E_{\text{covalent}}$  and  $E_{\text{non covalent}}$  are the total energy, covalent energy, and non-covalent energy respectively.

Now it can also expressed as,

$$E_{\text{total}} = E_{\text{bonds}} + E_{\text{angles}} + E_{\text{out-of-plane}} + E_{\text{dihedral}} + E_{\text{vander Waals}} + E_{\text{electrostatic}} \quad (8)$$

Where

$$E_{\text{covalent}} = E_{\text{bonds}} + E_{\text{angles}} + E_{\text{out-of-plane}} + E_{\text{dihedral}} \quad (9)$$

$$E_{\text{non covalent}} = E_{\text{vander Waals}} + E_{\text{electrostatic}} \quad (10)$$

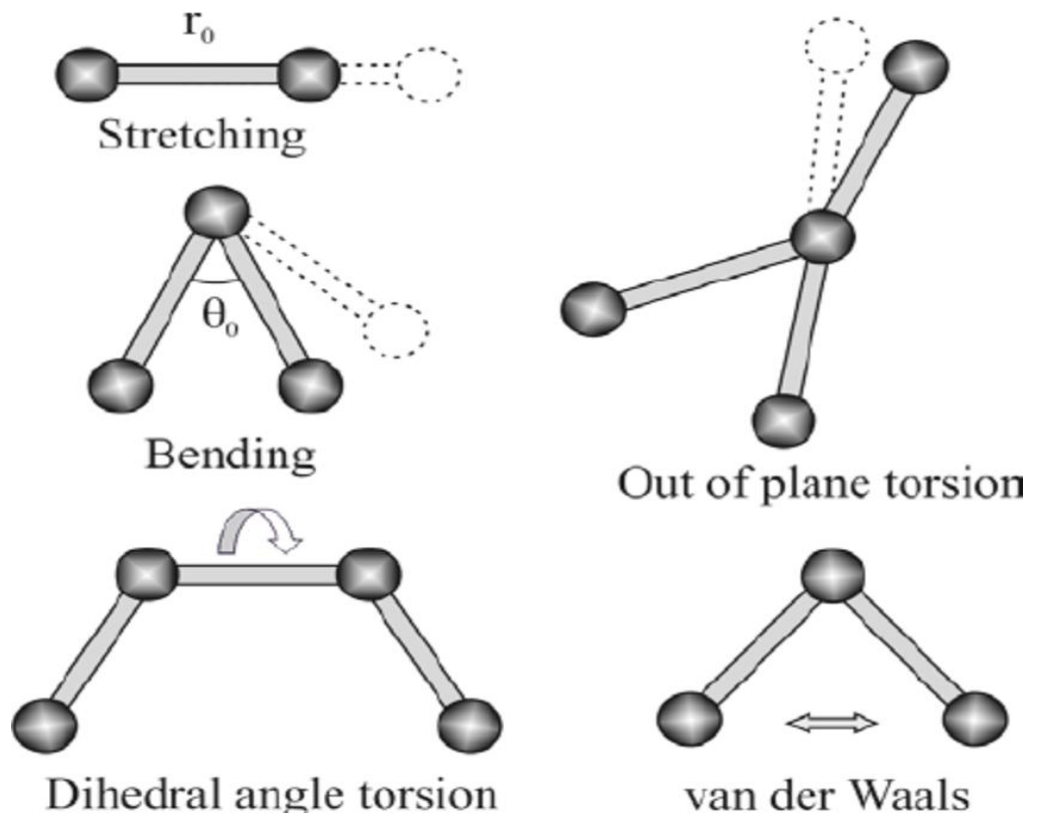


**Figure 3.2 Force-field degrees of freedom**

The interaction between hydrogen molecules and carbon atoms was modeled by using Lennard-Jones (LJ) potential which is given below

$$E_{ij} = 4\epsilon_{ij} \left[ \left( \frac{\sigma_{ij}}{r_{ij}} \right)^{12} - \left( \frac{\sigma_{ij}}{r_{ij}} \right)^6 \right] \quad (11)$$

Here  $E_{ij}$  is the pairwise total interaction energy and  $\epsilon_{ij}$  are the well-depth energy and  $\sigma_{ij}$  are the distance at which pairwise interaction energy goes to zero. And  $\sigma_{ij}$  and  $\epsilon_{ij}$  was calculated as the arithmetic mean of the value of the respective atom and the geometric mean of the value of the respective atom types respectively.

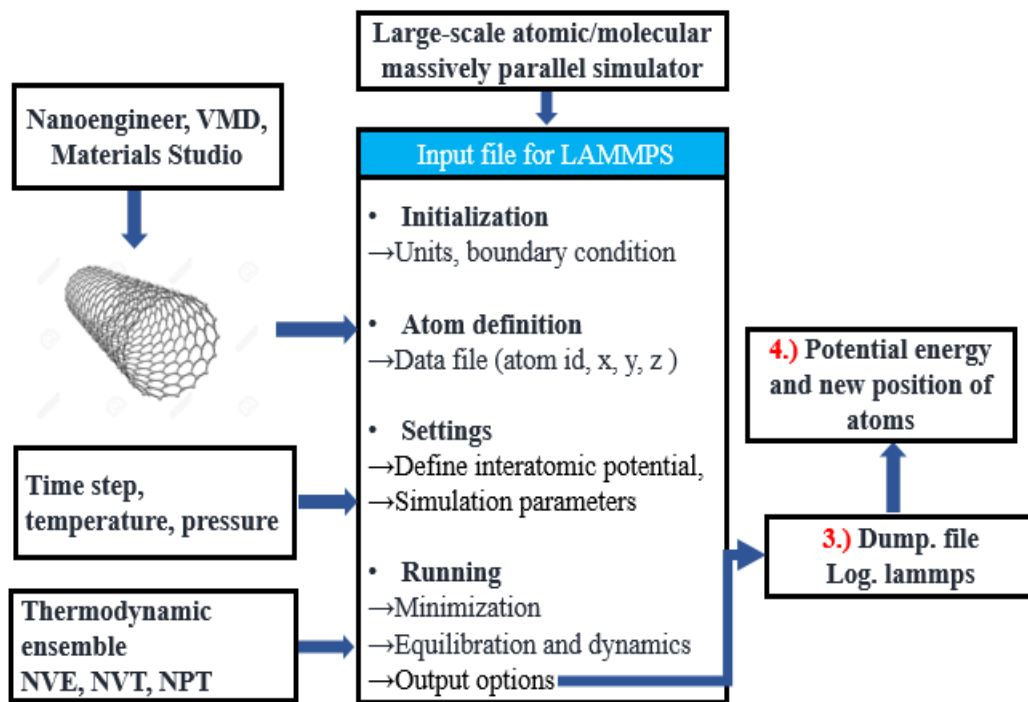


**Figure 3.3 Molecular dynamic simulation flow chart**

### 3.5 Equation of Motion

Molecular dynamics simulation solves equations of motion,  $F = ma$  i.e. Newton's second law in numerical way using integration algorithms, where  $F$  is the force exerted on the atoms,  $m$  is mass and  $a$  is acceleration. Now from here we can calculate the acceleration of each atom in the system if the force of each atoms is known. Integration of the equation of motion gives trajectory



that describes the positions, velocities, and accelerations of the atoms with respect to time. The state of the system can be predicted at any time if the positions and velocities of each atom are known.

Equation of motion i.e. Newton's second law is shown below [74],

$$\mathbf{F}_i = \mathbf{m}_i \frac{d^2 \mathbf{r}_i}{dt^2} = \frac{d\mathbf{v}}{dt} = \mathbf{m}_i \mathbf{a}_i \quad (12)$$

Where  $\mathbf{F}_i$ ,  $\mathbf{m}_i$  and  $\mathbf{a}_i$  is the force exerted, mass and acceleration of the  $i^{\text{th}}$  particle in the system respectively.

Force can also be defined as the gradient of the potential energy,

$$\mathbf{F}_i = - \frac{\partial E_i}{\partial \mathbf{r}_i} \quad (13)$$

Where  $E_i$  and  $\mathbf{r}_i$  are the potential energy and position of  $i^{\text{th}}$  particle respectively.

From above two equations yields

$$\mathbf{F}_i = - \frac{\partial E_i}{\partial \mathbf{r}_i} = \mathbf{m}_i \frac{d^2 \mathbf{r}_i}{dt^2} \quad (14)$$

Now the equation of motion have relation between the derivatives of the potential energy to the changes in position with respect to time.

If we take as the acceleration is constant than,

$$\mathbf{a} = \frac{d\mathbf{v}}{dt} \quad (15)$$

Velocity after integration,

$$\mathbf{v} = \mathbf{a}t + \mathbf{v}_0 \quad (16)$$

And we know that

$$\mathbf{v} = \frac{d\mathbf{r}}{dt} \quad (17)$$

Position after integration,

$$\mathbf{r} = \mathbf{v}t + \mathbf{r}_0 \quad (18)$$

Combining the above two equation for the expression of velocity and position we get value of  $\mathbf{r}$  at time  $t$  is shown below,

$$\mathbf{r} = \mathbf{a}t^2 + \mathbf{v}_0 t + \mathbf{r}_0 \quad (19)$$

Now acceleration is also defined as the derivative of the potential energy as shown below,

$$\mathbf{a} = - \frac{1}{m} \frac{dV}{d\mathbf{r}} \quad (20)$$

The initial positions of the atoms, an initial velocities and the acceleration which is determined by the gradient of the potential energy that gives trajectory of the particles. The positions and velocities at any times  $t$  is determined with the help of the positions and the velocities at time zero using the equation of motion.

The initial velocities of atoms are usually determined from a random distribution which is required to the temperature magnitudes and corrected so that overall momentum is zero is shown in the expression below.

$$\mathbf{P} = \sum_{i=1}^N m_i \mathbf{v}_i = \mathbf{0} \quad (21)$$

### 3.6 Methods of Controlling Pressure and Temperature

The pressure is controlled when the volume can change but the shape of the cell is not changed with the help of Berendsen and Andersen methods. And pressure and stress both can be controlled when the shape of the cell is changed by using Parrinello- Rahman method.

Temperature is a state variable which is thermodynamic state of the system and it is frequently used in molecular dynamics simulations. Temperature is related to the microscopic representation of dynamics simulations through the kinetic energy which is determined by the atomic velocities. The atomic velocities and the temperature in a system are related through the Maxwell-Boltzmann equation [75]. There are some methods for temperature control such as direct velocity scaling, Berendsen and Langevin thermostat and Nose-Hoover dynamics and Andersen methods.

### 3.7 Process for hydrogen storage in carbon nanotubes

Molecular dynamics (MD) is a computer simulation method for investigating the physical movements of atoms and molecules. Molecular dynamics is the most comprehensive molecular simulation method which determine the motions of individual molecules. Study the influence of both pristine and Polycrystalline carbon nanotubes with length ranging from 50 Å to 100 Å and diameter ranging from 15 Å to 21 Å were considered. Hydrogen storage and adsorption hydrogen energy in CNTs are determined with considering the effect of temperature at 77K, 100K, 200K, 273K, and pressure ranging from 0 bar to 40 bar was also studied [76].

Firstly, hydrogen molecules were randomly added surrounding the carbon nanotubes was modeled which is carried out by MDS and Perfect carbon nanotubes lattices were modeled separately using Materials Studio [77] and then imported into the simulation box. Stress-free nanotubes at a given temperature and pressure is taken for modeling the carbon nanotubes structures and then carbon nanotubes is surrounded by hydrogen molecules randomly.

Periodic boundary conditions is applied in-plane directions for eliminating the free edge defects and out-of-plane direction was applied with periodic boundary conditions with large dimensions to avoid any interlayer interactions of atoms in Carbon nanotubes in all MD calculations. Carbon nanotubes placed in the middle of the simulation box and carbon nanotubes is surrounded by hydrogen molecules randomly as shown in Fig. 3.4 By using Tersoff potential, the interatomic interaction of the carbon atoms in carbon nanotubes was modeled [78] and it can also predict the properties of carbon nanotubes successfully [79].

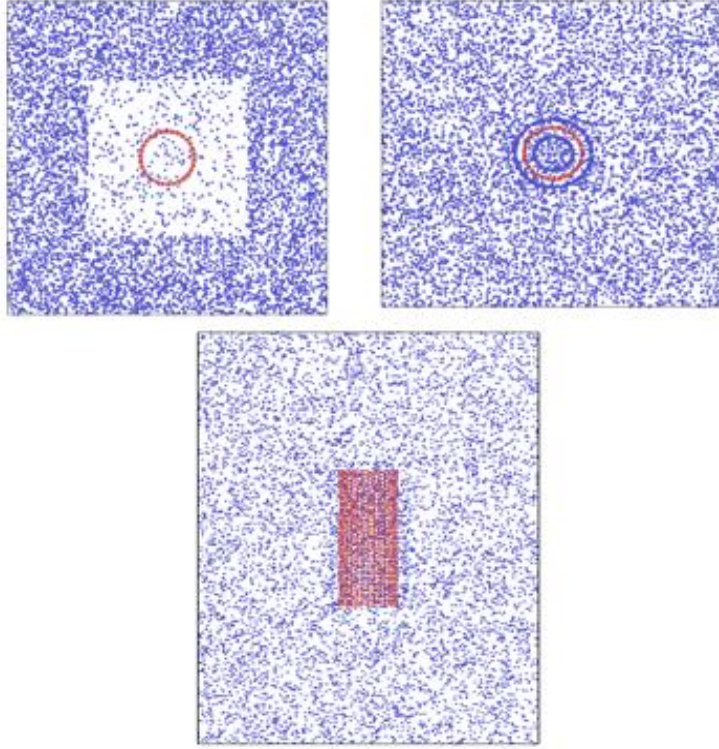


**Figure 3.4 System configuration of carbon nanotubes for H<sub>2</sub> molecules at Initial system configuration with relaxed carbon nanotubes at t=0sec, at simulation time 1 ns and adsorbed H<sub>2</sub> molecules around carbon nanotubes.**

The potential energy (E) of an atomic structures is a function of the distance  $r_{ij}$  between two adjacent atoms  $i$  and  $j$  in Tersoff potential is shown below,

$$E = \sum_i E_i = \frac{1}{2} \sum_{i \neq j} V_{ij} \quad (22)$$

Where,

$$V_{ij} = f_c(r_{ij})[f_R(r_{ij}) + b_{ij}f_A(r_{ij})] \quad (23)$$

$$f_R(r) = A \exp(-\lambda_1 r) \quad (24)$$

$$f_A(r) = -B \exp(-\lambda_2 r) \quad (25)$$

$$f_c(r) = \begin{cases} 1, & r < R - D \\ \frac{1}{2} - \frac{1}{2} \sin\left(\frac{\pi}{2} \frac{r - R}{D}\right), & R - D < r_{ij} < R + D \\ 0, & r_{ij} > R + D \end{cases} \quad (26)$$

$$b_{ij} = (1 + \beta^n \zeta_{ij}^n)^{-\frac{1}{2n}} \quad (27)$$

$$\zeta_{ij} = \sum_{k \neq i, j} f_c(r_{ik}) g(\theta_{ijk}) \exp[\lambda_3^m (r_{ij} - r_{ik})^m] \quad (28)$$

$$g(\theta) = \gamma_{ijk} \left( 1 + \frac{c^2}{d^2} - \frac{c^2}{[d^2 + (\cos \theta - \cos \theta_0)^2]} \right) \quad (29)$$

Where  $V_{ij}$ ,  $f_R$  and  $f_A$  is the potential energy of the pair, repulsive and attractive pair potentials respectively with  $f_c$  as a cut off function. Sometime  $f_R$  and  $f_A$  is also referred as a two-body term, and three-body interactions respectively.

Term  $b_{ij}$  is the many-body parameter that expressed how the bond formation energy is affected due to the presence of adjacent atoms. The interaction between hydrogen molecules and carbon atoms in carbon nanotubes which is based on physisorption was modeled by using Lennard-Jones (LJ) potential which is discussed below,

$$u_{ij} = 4\varepsilon_{ij} \left[ \left( \frac{\sigma_{ij}}{r} \right)^{12} - \left( \frac{\sigma_{ij}}{r} \right)^6 \right] \quad (30)$$

Where  $u_{ij}$ ,  $\varepsilon_{ij}$  and  $\sigma_{ij}$  is the pairwise interaction energy, the well-depth energy and the distance at which pair interaction energy goes to zero, respectively and 12 Å is cut-off distance for LJ interactions. LJ interaction parameters for carbon atoms and hydrogen molecules as shown in **table 3.1** [80]. Carbon atoms and hydrogen molecules interactions i.e.  $\sigma_{ij}$  and  $\varepsilon_{ij}$  were obtained as the arithmetic mean of the value of the respective atom and the geometric mean of the value of the respective atom types respectively by using Lorentz-Berthelot mixing rules,

$$\varepsilon_{ij} = \sqrt{\varepsilon_{ii}\varepsilon_{jj}} \quad \sigma_{ij} = \frac{\sigma_{ii} + \sigma_{jj}}{2} \quad (31)$$

**Table 3.1 Lennard-Jones interaction parameters for carbon atoms and hydrogen molecules.**

Parameter	H <sub>2</sub> -H <sub>2</sub>	C-C	C- H <sub>2</sub>
$\epsilon$ [Kcal/mol]	0.067962	0.055641	0.0636932
$\sigma$ [Å]	0.296	0.340	3.179

Considering the van der Waals interactions molecular dynamic simulation was run using LAMMPS to optimize the system parameters and the van der Waals interactions were modelled by Lennard-Jones (LJ) model. LJ potential parameters for carbon and hydrogen molecules were derived from experiment data of hydrogen and graphene. Timestep size of 0.5 femtoseconds was considered for the hydrogen adsorption in molecular dynamic simulation. The energy minimization in carbon nanotubes was applied with an energy convergence of  $10^{-10}$  to obtain using the conjugate gradient method. After energy minimization, the system was equilibrated for 250 picosecond under isothermal and isobaric conditions to produce a stress-free nanotubes in planar directions and carbon nanotubes is surrounded by hydrogen molecules randomly in the simulation box side by side, above and below the carbon nanotubes.

The number of hydrogen molecules added to the system was randomly chosen to be about 4 hydrogen molecules per carbon atom in the carbon nanotubes and to achieve the desired system temperature and pressure, system ran for 250 picosecond. After that, an equilibration run of 4 nanosecond was performed under the isothermal and isobaric conditions and then take a long equilibration step is achieved to establish an equilibrated system with uniform distribution in the system and to get the hydrogen gravimetric capacity and adsorption hydrogen energy in carbon nanotubes. The above simulation steps was execute multiple times for different set of pressure and temperature.

The hydrogen adsorbed in carbon nanotubes was determined by observing the distribution of potential energy of each atoms and the gravimetric density (wt. %) of hydrogen molecules was calculated by

$$\delta(\text{wt}\%) = \frac{w_{H_2-\text{adsorbed}}}{w_{H_2-\text{adsorbed}} + w_{c-\text{nanotube}}} \quad (32)$$

Where,  $w_{H_2-\text{adsorbed}}$  is the weight of adsorbed hydrogen molecules and  $w_{c-\text{nanotube}}$  is the weight percentage of the carbon nanotubes.

The hydrogen adsorption energy in carbon nanotubes was calculated by

$$E_{\text{adsorption}} = E_{\text{carbon nanotube}+H_2} - (E_{\text{carbon nanotube}} + E_{H_2}) \quad (33)$$

Where  $E_{\text{carbon nanotube}}$  is the potential energy of carbon nanotubes,  $E_{H_2}$  is the potential energy of one hydrogen molecule and  $E_{\text{carbon nanotube}+H_2}$  is the potential energy of the carbon nanotube with adsorbed hydrogen molecules.

### 3.8 Adsorption isotherm equations

Hydrogen adsorption behavior between adsorbate and adsorbent at different pressures and temperature should be explain in various analytic expressions of adsorption isotherms. These equations define the adsorption density ( $q$ ) of the adsorbent as a function of pressure ( $p$ ) for a specific temperature.

#### 3.8.1 Langmuir Isotherm

The Langmuir [81] theory assumes that the adsorbate stick to the adsorbent and covers the surface forming a monolayer of the adsorbate and it is also assumes that adsorption to be homogeneous. Dense state allows the higher volumes to be stored by sorption which is possible by compression at low pressures.

$$q = \frac{q_{mL}K_L p}{1 + K_L p} \quad (34)$$

Where,  $q$  is the amount of adsorbate on the surface adsorbent at a pressure  $p$

And  $q_{mL}$  is the constant reflecting theoretical monolayer capacity and  $K_L$  is the Langmuir constant which shows the strength of adsorption.

### 3.8.2 Freundlich Isotherm

Freundlich isotherm [82] refers to that surface which is heterogeneity and the exponential distribution of adsorption sites and their energies. And the expression which is applied to heterogeneous adsorption and it is given by

$$q = K_L p^{n_F} \quad (35)$$

Where  $K_L$  and  $n_F$  is the Freundlich constant and the heterogeneity factor respectively.

### 3.8.3 Sips (Langmuir–Freundlich) Isotherm

The Sips isotherm [83] is defined as a combination of the Langmuir and Freundlich isotherms and its expression is given by,

$$q = \frac{q_{mS} K_S p^{n_S}}{1 + K_S p^{n_S}} \quad (36)$$

Where  $q_{mS}$ ,  $K_S$  and  $n_S$  is maximum adsorption capacity at a temperature, the Sips constant and the heterogeneity factor respectively. If  $n_S$  is equal to 1, then Sips equation becomes the Langmuir equation and the surface is homogeneous.

### 3.8.4 Fritz–Schlunder Isotherm

The Fritz–Schlunder isotherm [84] expression is given by,

$$q = \frac{q_{mFS} K_{FS} p}{1 + q_{mFS} p^{n_{FS}}} \quad (37)$$

Where  $q_{mFS}$  is a constant reflecting maximum adsorption capacity ( $\text{mg g}^{-1}$ ),  $K_{FS}$  and  $n_{FS}$  is the Fritz–Schlunder equilibrium constant and the Fritz–Schlunder model exponent respectively.

## 3.9 Modeling polycrystalline carbon nanotubes

Polycrystalline carbon nanotubes were created by rolling graphene sheets containing grainboundaries. The atomic structures of the graphene sheets is randomly distributed with grain sizes and shapes will be created by using Voronoi tessellation technique [85, 86]. The systematic steps to create a



polycrystalline carbon nanotubes by rolling the graphene sheet with randomly distributed grain boundaries is involved here as shown in fig.3.5 and it shows that the generated a collection of polygons separated by planar cell walls perpendicular lines to connect neighbouring nucleation sites. We constructed a polycrystalline graphene sheet by filling each cell with randomly oriented graphene domains and atoms adjacent to the planar cell walls produce the grain boundaries.

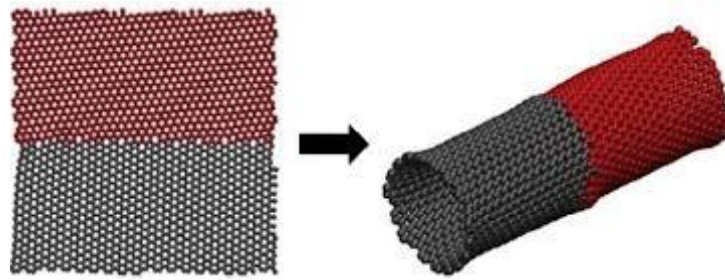


**Figure 3.5: Formations of polycrystalline carbon nanotubes using graphene sheets**

Inside the polycrystalline graphene with dimensions of  $100 \text{ \AA} \times 100 \text{ \AA}$  were selected at several regions at different locations and extracted to create the basic structure then it is rolled to form polycrystalline carbon nanotubes. The different arrangements can be generated along the grain boundaries such as pentagon, heptagon, quadrilaterals, octagons, and nonagons defects [86] and all arrangements should be considered for determining the hydrogen storage and hydrogen adsorption energy in polycrystalline carbon nanotubes using molecular dynamic simulation.

### **3.10 Process of hydrogen storage considering strain**

Hydrogen storage and hydrogen adsorption energy can be determined with consideration of the effects of strain in carbon nanotubes using molecular dynamic simulation. Strain can modify the thermal conductivity, atomic structure, chemical activity, lattice vibration, and mechanical properties in 2D nanomaterials. We can apply mechanical strain which is varying from 0% to 7% at specific temperature and pressure in carbon nanotubes to study its effects

on adsorption of hydrogen molecules and it is signify to sustain metal atoms on carbon-based substrate .Over 15% of strain can be easily implement in carbon nanotubes as demonstrated the experimentally.

Calculating the strain, expression is given by

$$\text{Strain} = \frac{\text{strain rate} \times \text{timestep} \times \text{run time}}{\text{Actual length}} \quad (38)$$

Here, time step is in Picosecond and actual length of carbon nanotubes is in Angstrom (Å).

The time step is known as the length of time between two successive iterations in an molecular dynamic simulation and smaller time steps may increase the accuracy of the simulation but larger time steps increase the computational efficiency. So, the time step controls the trade-off between accuracy and computational efficiency in an molecular dynamic simulation. In this section, time step is taken as .0005 picosecond and strain rate is vary according to the corresponding strain (0% to7%) is applying in the direction of length of the carbon nanotubes and here length is taken as 81 Å and run time is also vary according to the strain rate in the simulation for determined the hydrogen storage and hydrogen adsorption energy.

Weight percent of hydrogen adsorption was determined for the pristine carbon nanotube at different temperature and pressure using molecular dynamics simulations. The several simulations performed in this study suggest that hydrogen molecules are physically surrounded around the pristine carbon nanotubes, as shown in Figure 4.1.

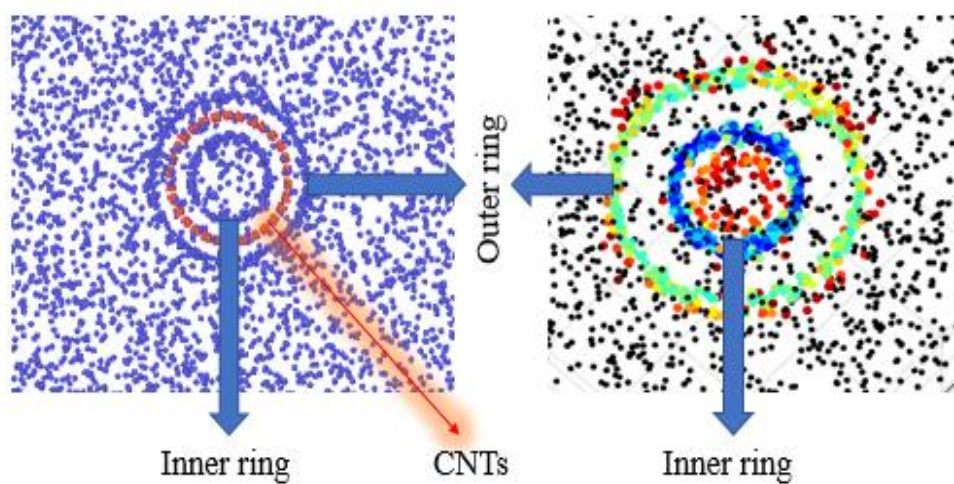


**Figure 4.1** Simulation image for hydrogen storage in carbon nanotubes

Simulations in molecular dynamics for adsorption phenomenon can achieved an equilibrated system and these system with equilibrated potential energy, temperature, and pressure indicates a stable system. For the desired temperature and pressure it can be observed that the system was stable and equilibrated throughout the simulation. The intermolecular interaction of the hydrogen molecules are repels to each other as more and more hydrogen are surrounded around the pristine carbon nanotubes. But hydrogen molecules are adhere to low potential energy sites and it bring the whole system to an equilibrium and in stable.

Hydrogen adsorption density was determined with potential energy distribution (PED) patterns of hydrogen molecules were observed and hydrogen molecules are adsorbed around the pristine carbon nanotubes had lower potential energy as compared to free hydrogen molecules on the basis for adsorption percentage estimation. Potential energy distribution of each

hydrogen molecules around the pristine carbon nanotubes at 77K and 1 MPa with a probabilistic curve fitting as shown in fig. It was indicate that a local minima point exists in the potential energy distribution below this minimum point where adsorbed hydrogen molecules is lie as shown in Figure 4.2 (a). Hydrogen molecules belonging to the adsorbed potential energy for validation of the estimation method were segregated and hydrogen molecules are surrounded around the pristine carbon nanotubes as shown in Figure 4.2 (b).

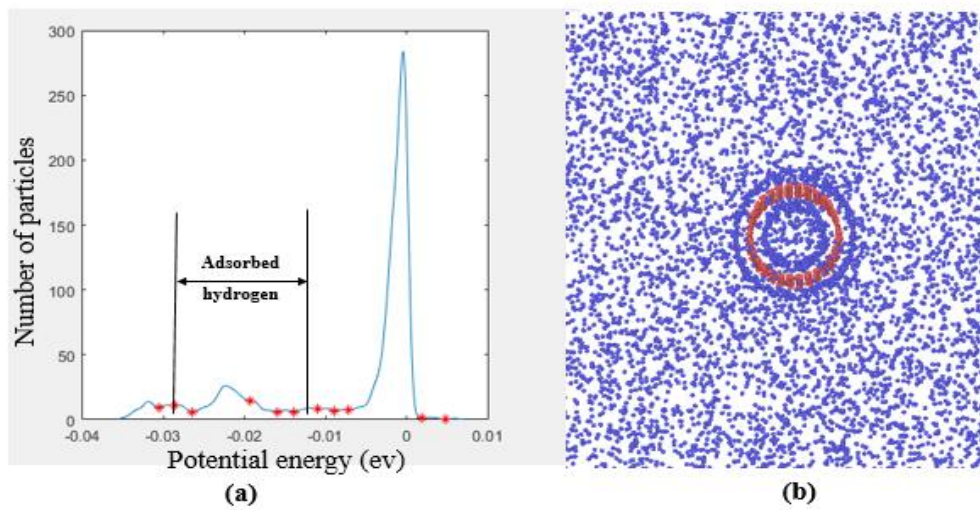


**Figure 4.2 (a) Potential Energy Distribution (PED) of hydrogen molecules and (b) front view and top view of the hydrogen molecules at 77 K and 1 MPa.**

Carbon atoms are kept hidden for clarity in carbon nanotubes and then the number of adsorbed hydrogen molecules were counted and adsorption weight percentage was calculated using the Eq. 32. Average of the weight percentage for the last few time steps simulations of the equilibrated system was calculated to get an approximate hydrogen adsorption value. No other study has used this method to observe adsorption phenomena using MDS according to the best of the authors' knowledge and using this method for estimating adsorption weight percentage for the hydrogen adsorption phenomenon was studied on multiple systems of a carbon nanotubes and hydrogen molecules were studied and the hydrogen adsorption energy (ev) of the hydrogen molecules was also calculated.

#### 4.1 Hydrogen adsorption weight percent and hydrogen adsorption energy for pristine carbon nanotubes

Hydrogen adsorption weight percentage was determined for the pristine carbon nanotubes using the potential energy distribution patterns of  $H_2$  molecules is adsorbed around the carbon nanotubes. Hydrogen adsorption Weight percentage was calculated at 20 bar pressure and at different temperature 77 K, 100 K, 200K, 273K as shown in Figure 4.3 and Figure 4.3(a) shows that as the operating temperature increases the hydrogen adsorption capacity decreases due to increase in thermal motion of hydrogen molecules and also we can see that at lower temperature van der waals interaction for the hydrogen gas molecules and pristine carbon nanotubes are very strong and as temperature increases the van der waals interaction decreases and then due to the strong interaction forces hydrogen adsorption density of hydrogen molecules are higher at lower temperature. The results obtained for the weight adsorption density of hydrogen molecules for pristine carbon nanotubes at different temperature at 20 bar pressure as shown in Table 4.1.

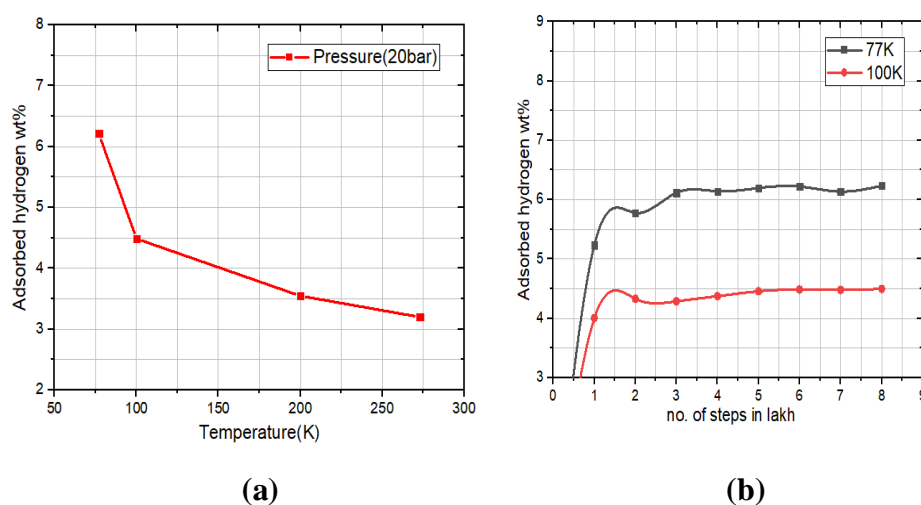


**Figure 4.3 Variation of hydrogen adsorption capacity (wt %) for pristine Carbon nanotube at constant pressure (20bar) (a) at different temperature (b) with different no. of steps (lakh) at 77k and 100 K.**

And Figure 4.3(b) shows that as the no. of steps in lakh for the simulations in molecular dynamics is increases then at initial stage weight percentage of the pristine carbon nanotubes is vary but after reaching at a saturation level weight percentage of adsorbed hydrogen molecules is approximately equal, hence we

can find that the minimum 5 to 6 lakh no. of steps for the simulations to get accurate result for calculating the hydrogen adsorption capacity.

**Table 4.1 Weight adsorption density of hydrogen molecules for pristine carbon nanotubes at different temperature at 20 bar pressure**

Temperature (k)	77K	100K	200K	273K
Weight percentage	6.2144	4.4860	3.5461	3.1968

Hydrogen adsorption density was calculated using the data obtained for the pristine carbon nanotubes using the potential energy distribution for hydrogen molecules are adsorbed around the carbon nanotubes for different pressure ranging from 1 bar to 40 bar (4MPa) and at different temperature 77 K, 100 K, 200K, 273K as shown in Figure 4.4. Due to the effect of pressure, here we can see that as the pressure increases the gravimetric hydrogen density increases because at a higher density of hydrogen molecules adheres to the adsorbent upon increasing the pressure. At 2 bar pressure the gravimetric density is 6.0958, 4.4492, 3.3281, 3.2433 and at 10 bar pressure 6.178, 4.4872 ,3.972 ,3.7877 at temperature 77 K, 100K, 200K, 273K respectively.

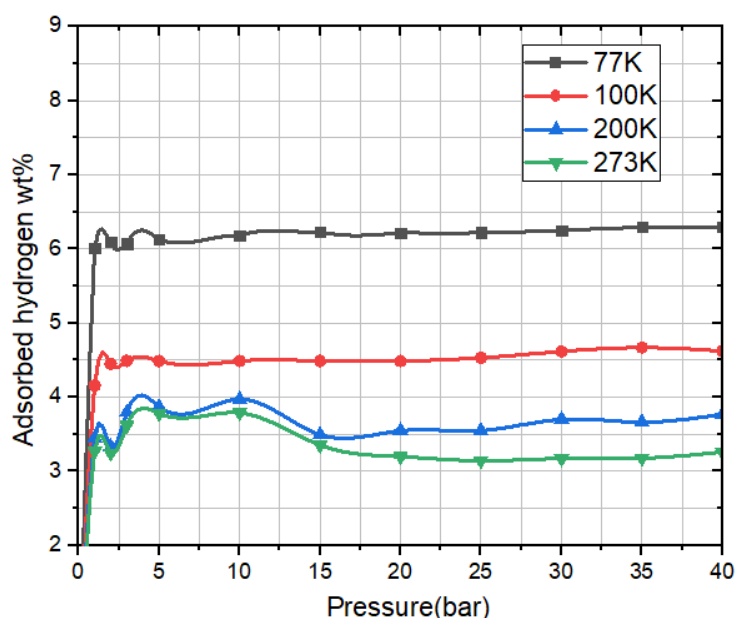


**Figure 4.4 Variation of adsorption hydrogen wt% of Pristine carbon nanotubes with pressure at different temperature.**

And as the pressure is increased the hydrogen gravimetric capacity increases rapidly but after reaching a certain pressure value it reaches a saturation level. Due to the effect of the temperature, as the temperature increases the gravimetric hydrogen density of hydrogen molecules are decreases because of hydrogen molecules are weakly bonded van der Waals interaction with pristine carbon nanotubes and also due to the kinetic energy of the system increases and as a result, hydrogen adsorption density of hydrogen molecules is decreases at higher temperature and then due to the strong interaction forces hydrogen adsorption density of hydrogen molecules are higher at lower temperature [87].

Adsorption hydrogen energy (ev) was calculated using the data obtained for the pristine carbon nanotubes for hydrogen molecules for different pressure ranging from 1 bar to 40 bar (4MPa) and at different temperature 77 K, 100 K, 200K, 273K as shown in Figure 4.5.

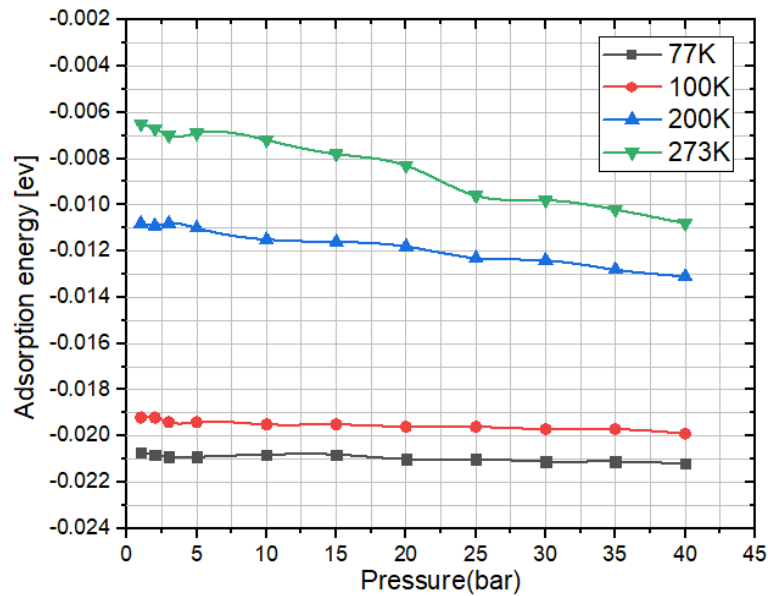


**Figure 4.5 Variation of adsorption hydrogen energy (eV) for Pristine carbon nanotubes with pressure at different temperature.**

Here we can see that the adsorption energies are calculated in negative values and it signifies that the strength of the attraction between hydrogen molecules and pristine carbon nanotubes and a higher value adsorption hydrogen energy signifies a stronger attractive force between the adsorbate and adsorbent. If the pressure increases we can observed that the hydrogen adsorption energy



reduces to a more negative value indicating that the stronger adsorption between the pristine carbon nanotubes and hydrogen molecules. It is observed that at higher temperatures an indicating a weaker adsorption strength due to increase in adsorption energy and at lower temperatures, adsorption strength is strong then adsorption energy is decreases.

#### 4.2 Hydrogen adsorption weight percent and hydrogen adsorption energy for Polycrystalline carbon nanotubes

Weight percent of hydrogen adsorption for the polycrystalline carbon nanotubes i.e. carbon nanotubes containing grain boundary was calculated using the data obtained for hydrogen molecules are adsorbed around the polycrystalline carbon nanotubes for different pressure ranging from 1 bar to 40 bar (4MPa) and at different temperature 77 K, 100 K, 200K, 273K as shown in Figure 4.6.

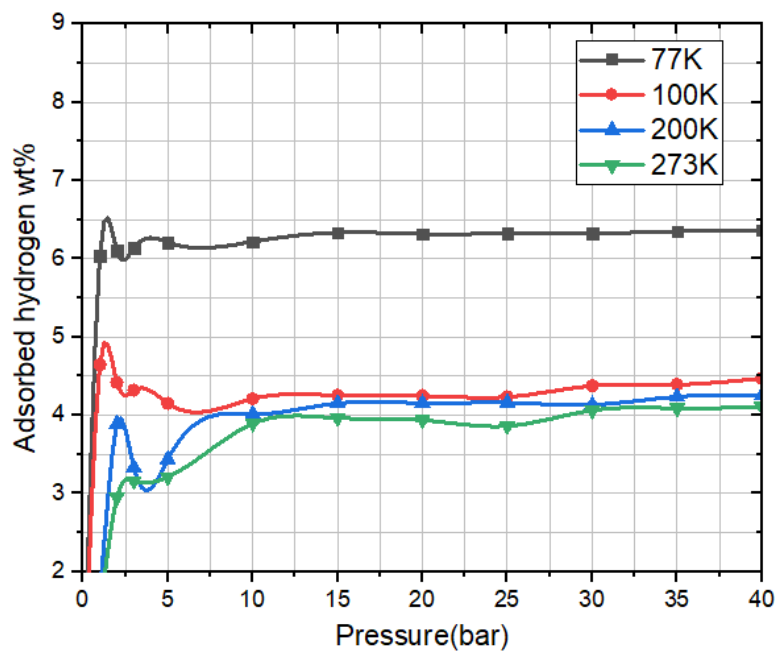


**Figure 4.6 Variation of adsorption hydrogen wt% for Polycrystalline CNTs with pressure at different temperature.**

Here we can observed that the hydrogen adsorption density of carbon nanotubes containing grain boundary is more than that of the pristine carbon nanotubes because of grain boundary creating in carbon nanotubes there is formation of some defects in carbon nanotubes and due to these defects



hydrogen molecules are adsorbed more as compare to pristine carbon nanotubes. Here we can see that as the pressure increases the gravimetric density (GD) of hydrogen increases because at a higher density of hydrogen molecules adheres to the adsorbent upon increasing the pressure and as the pressure is increased the hydrogen gravimetric capacity increases rapidly but after reaching a certain pressure value it reaches a saturation level. At 2 bar pressure the gravimetric density is 6.1019, 4.4192, 3.8883, 2.9507 and at 40 bar pressure 6.364, 4.4712 ,4.2529 ,4.1084 at temperature 77 K, 100K, 200K, 273K respectively. As the temperature increases the gravimetric hydrogen density of hydrogen molecules are decreases because of the hydrogen molecules are weakly bonded van der Waals interaction with pristine carbon nanotubes and also due to the kinetic energy of the system increases. At 10 bar pressure the gravimetric density is 6.2175, 4.2113, 4.0131 and 3.8929 at temperature 77 K, 100K, 200K, 273K respectively.

Adsorption hydrogen energy (ev) was determined using the data obtained for the polycrystalline carbon nanotubes i.e. carbon nanotubes containing grain boundary for hydrogen molecules for different pressure ranging from 1 bar to 40 bar (4MPa) and at different temperature 77 K, 100 K, 200K, 273K as shown in Figure 4.7.

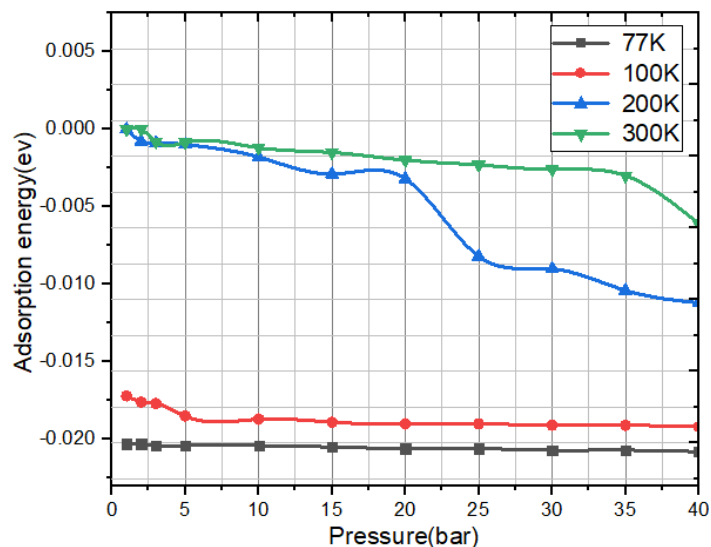


**Figure 4.7 Variation of adsorption hydrogen energy (ev) for Polycrystalline carbon nanotubes with pressure at different temperature.**

Here we can see that the adsorption energies are calculated in negative values and adsorption energy is less as compare to pristine carbon nanotubes because of grain boundary creating in carbon nanotubes there is formation of some defects in carbon nanotubes and due to these defects adsorption strength of hydrogen molecules is strong then adsorption energy is decreases. Higher value adsorption hydrogen energy signifies a stronger attractive force between the adsorbate and adsorbent. If the pressure increases we can observed that the hydrogen adsorption energy reduces to a more negative value indicating that the stronger adsorption between the polycrystalline carbon nanotubes containing grain boundary and hydrogen molecules. It is observed that at higher temperatures an indicating a weaker adsorption strength due to increase in adsorption energy.

Weight percent of hydrogen adsorption for the polycrystalline carbon nanotubes i.e. carbon nanotubes containing grain boundary was compared with pristine carbon nanotubes and it was calculated using the data obtained for hydrogen molecules are adsorbed around the polycrystalline carbon nanotubes and pristine carbon nanotubes for different pressure ranging from 1 bar to 40 bar (4MPa) and at temperature 77 K as shown in Figure 4.8 as the comparison between pristine and polycrystalline carbon nanotubes.

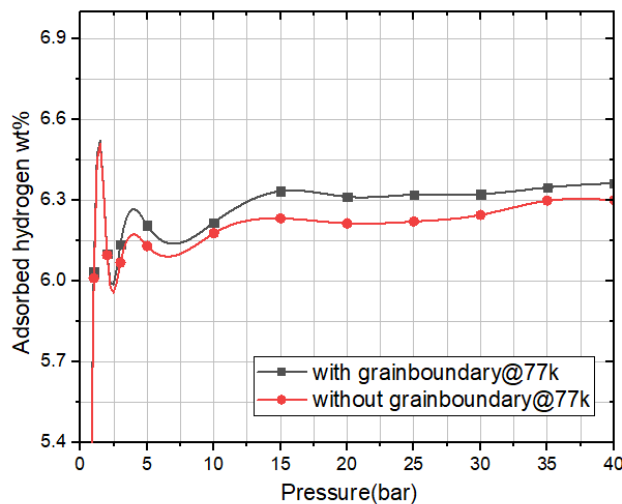


**Figure 4.8 Hydrogen adsorption wt% comparison btw pristine and polycrystalline carbon nanotubes with different pressure at 77 K.**

Here we can observed that the hydrogen adsorption capacity of carbon nanotubes containing grain boundary is more than that of the pristine carbon nanotubes because of grain boundary creating in carbon nanotubes there is formation of some defects in carbon nanotubes and due to these defects hydrogen molecules are adsorbed more as compare to pristine carbon nanotubes. The results obtained for the weight adsorption density of hydrogen molecules for pristine and polycrystalline carbon nanotubes at 77K as shown in Table 4.2.

**Table 4.2 Weight adsorption density of hydrogen molecules for pristine and polycrystalline carbon nanotubes at 77K.**

<b>Pressure (bar)</b>	<b>Pristine CNTs</b>	<b>Polycrystalline CNTs</b>
1 bar	6.0104	6.0341
2 bar	6.0958	6.1019
3 bar	6.0686	6.1368
5 bar	6.1302	6.2072
10 bar	6.178	6.2175
15 bar	6.2331	6.3346
20 bar	6.2144	6.3133
25 bar	6.2212	6.3214
30 bar	6.2459	6.3233
35 bar	6.2985	6.3481
40 bar	6.3012	6.364

### 4.3 Hydrogen adsorption weight percent and hydrogen adsorption energy for both Pristine and Polycrystalline carbon nanotubes considering Strain

Weight percent of hydrogen adsorption was determined for both pristine and polycrystalline carbon nanotube considering Strain at different temperature and pressure using molecular dynamics simulations. The several simulations performed in this study suggest that hydrogen molecules are physically surrounded around the pristine and polycrystalline carbon nanotubes and adsorption weight percentage was calculated using the Eq. 32 and strain is calculated using the Eq. 38 and strain is determined in the direction of length of carbon nanotube in which length should be increase and diameter should be decrease as shown in Figure 4.9.

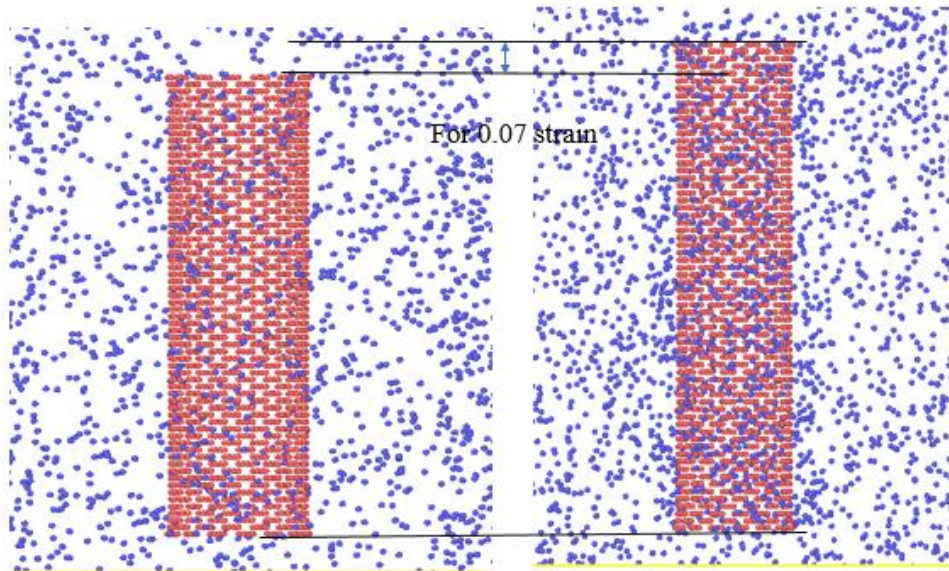


**Figure 4.9 Simulation image for hydrogen storage in CNTs Considering Strain**

Hydrogen adsorption weight percentage was determined for the pristine carbon nanotubes considering Strain using the potential energy distribution patterns of  $H_2$  molecules are adsorbed around the CNTs at 20 bar pressure and at temperature 77 K and 200 K at different strain ranging from 0.01 i.e. 1% to 0.07 i.e. 7% as shown in Figure 4.10 and here we can see that as the percentage of strain is increases adsorption weight percentage is also increased because bond length between carbon-carbon atom is increased due to stretched produced in carbon nanotubes by applying strain and then it creates a gap

between carbon atom and when strain is more than gap is also increased between carbon atom due to strain produced in CNTs and due to this gap more hydrogen molecules are adsorbed in carbon nanotubes.

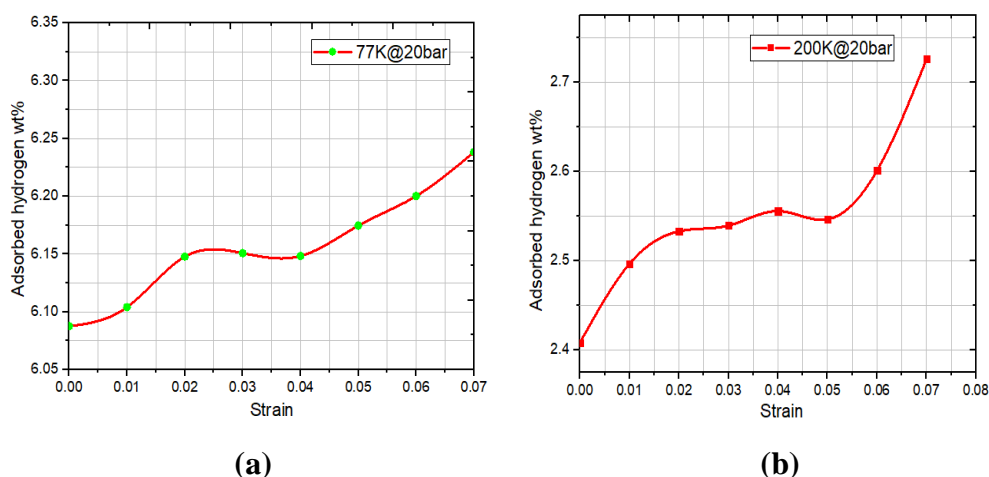


**Figure 4.10 Variation of adsorption hydrogen wt% of Pristine CNTs considering Strain with strain at 20 bar pressure (a) at 77K (b) at 200K.**

Figure 4.10(a) and Figure 4.10(b) show that as the temperature is increases adsorption weight percentage in carbon nanotubes is decreased due to increase in thermal motion of hydrogen molecules at temperature varying from 77K to 200K at 20 bar pressure. The results obtained for adsorption weight percentage of hydrogen molecules for pristine carbon nanotubes considering Strain at 77K and 20 bar pressure at different strain as shown in Table 4.3.

**Table 4.3 Weight adsorption density of hydrogen molecules for pristine carbon nanotubes at 77K and 20 bar Pressure**

Strain	0.0	0.01	0.02	0.03	0.04	0.05	0.06	0.07
wt%	6.0875	6.104	6.1477	6.1508	6.1483	6.1746	6.2002	6.2383

Adsorption hydrogen energy (ev) was calculated using the data obtained for the pristine carbon nanotubes considering Strain for hydrogen molecules at different strain ranging from 0.0 to 0.07 and at temperature 77K and 200K at 20 bar pressure as shown in Figure 4.11. Adsorption energies are calculated in negative values and it signifies that the strength of the attraction between H<sub>2</sub> molecules and pristine CNTs considering Strain. If the percentage of strain which is applied in carbon nanotubes is increased than we can observed that

the hydrogen adsorption energy reduces to a more negative value indicating that the stronger adsorption between the pristine carbon nanotubes considering strain and hydrogen molecules as shown in Figure 4.11(a). And it is also observed that at higher temperatures an indicating a weaker adsorption strength of hydrogen molecules in carbon nanotubes due to increase in adsorption energy and at lower temperatures adsorption strength of hydrogen molecules in carbon nanotubes is strong then adsorption energy is decreases as shown in Figure 4.11(b).

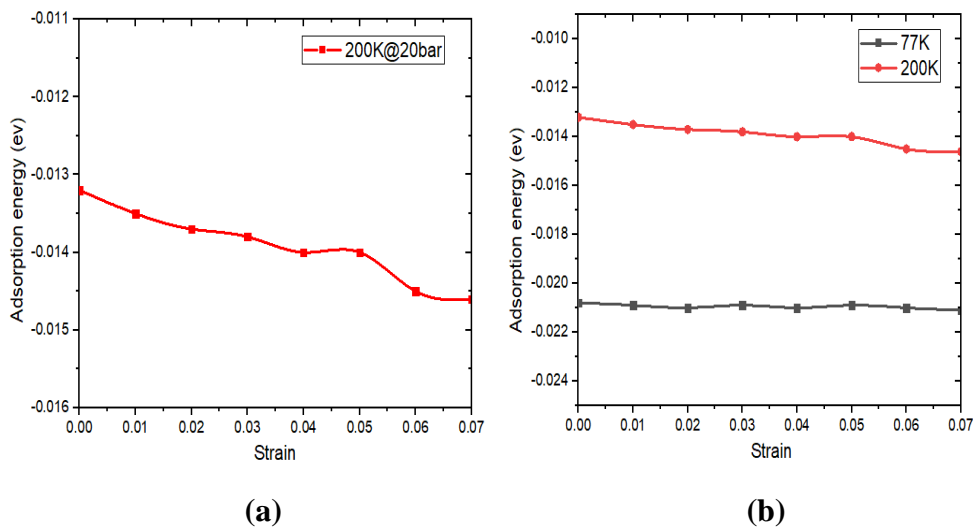


**Figure 4.11 Variation of adsorption hydrogen energy (eV) for Pristine CNTs considering Strain with different Strain at 20bar (a) at 200 K temperature (b) at 77K and 200K.**

Hydrogen adsorption weight percentage was determined for the polycrystalline carbon nanotubes considering strain using the potential energy distribution patterns of  $H_2$  molecules are adsorbed around the CNTs at 20 bar pressure and at temperature 77 K, 100K and 200 K at different strain ranging from 0.01 i.e. 1% to 0.07 i.e. 7% as shown in Figure 4.12 (a) and here we can see that as the percentage of strain is increases adsorption weight percentage is also increased because bond length between carbon-carbon atom is increased due to stretched produced in carbon nanotubes by applying strain and then it creates a gap between carbon atom and when strain is more than gap is also increased between carbon atom due to strain produced in CNTs and due to this gap more hydrogen molecules are adsorbed in carbon nanotubes.

And as the temperature is increases adsorption weight percentage in polycrystalline carbon nanotubes is decreased due to increase in thermal motion of hydrogen molecules at temperature varying from 77K to 200K at 20 bar pressure.

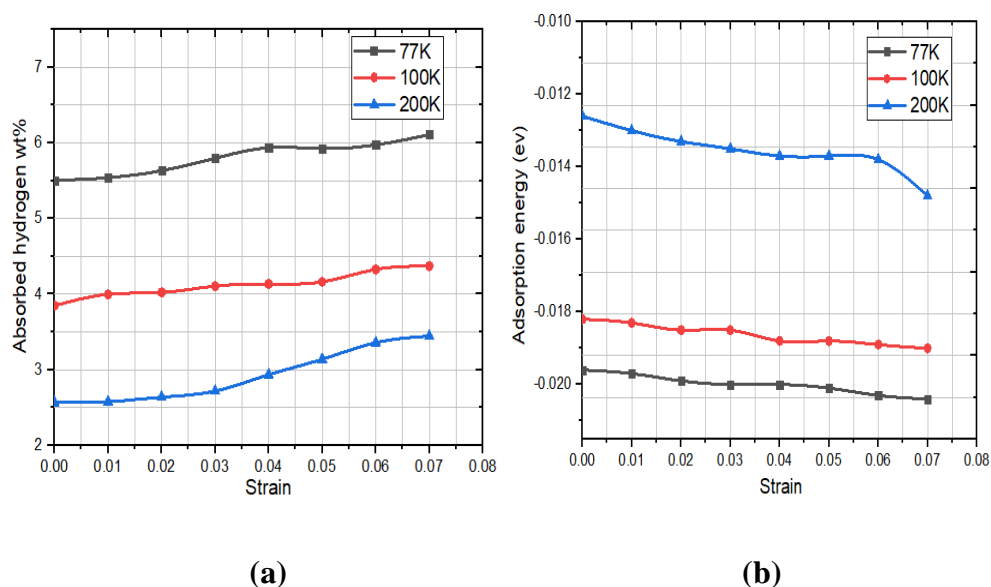


**Figure 4.12 Variation of (a) adsorption hydrogen wt% (b) hydrogen adsorption energy (ev) of polycrystalline carbon nanotubes with different strain at different temperature at 20 bar pressure.**

Adsorption hydrogen energy (ev) was calculated using the data obtained for the polycrystalline carbon nanotubes with considering Strain for hydrogen molecules at different strain ranging from 0.0 to 0.07 and at temperature 77K, 100K and 200K at 20 bar pressure as shown in Figure 4.12(b). Adsorption energies are calculated in negative values and it signifies that the strength of the attraction between  $H_2$  molecules and polycrystalline CNTs considering Strain. If the percentage of strain which is applied in polycrystalline carbon nanotubes is increased than we can observed that the hydrogen adsorption energy reduces to a more negative value indicating that the stronger adsorption between the polycrystalline carbon nanotubes considering strain and hydrogen molecules as shown in Figure 4.12(b). And it is also observed that at higher temperatures an indicating a weaker adsorption strength of hydrogen molecules in carbon nanotubes due to increase in adsorption energy and at lower temperatures adsorption strength of hydrogen molecules in carbon nanotubes is strong then adsorption energy is decreases.

Gravimetric density weight percent of hydrogen molecules for the carbon nanotubes considering 0.06 i.e. 6% Strain is compared with pristine carbon nanotubes and it is determined for different temperature i.e. 77K, 100K, 200K, 273K at 20 bar pressure as shown in Figure 4.13(a). Hydrogen adsorption weight percentage is compared between pristine and polycrystalline CNTs by applying different Strain at 200K at 20 bar pressure as shown in Figure 4.13(b). Here we can see that in both case there is improvement of hydrogen adsorption weight percentage by applying strain in both pristine and polycrystalline carbon nanotubes. Here we can observed that the hydrogen adsorption capacity of CNTs considering strain and polycrystalline carbon nanotubes considering strain is more than that of the pristine carbon nanotubes because there is creating a gap between carbon atom and due to this gap more hydrogen molecules are adsorbed in carbon nanotubes and the bond length between carbon-carbon atom is also increased by applying strain in carbon nanotubes and as the temperature is increases hydrogen adsorption weight percentage is decreased due to increase in thermal motion of hydrogen molecules and also at lower temperature van der waals interaction for the hydrogen gas molecules and carbon nanotubes are very strong. Hence at lower temperature hydrogen adsorption weight percentage is more.

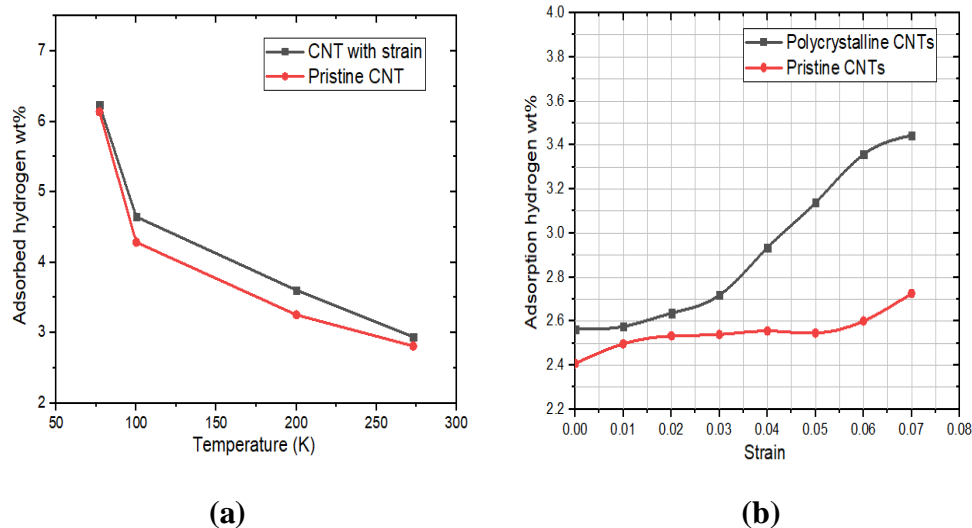


**Figure 4.13 Comparison the hydrogen adsorption wt% at 20 bar pressure between (a) pristine CNTs and CNTs with Strain (6%) at different temperature (b) pristine and polycrystalline CNTs with different Strain at 200K temperature.**



#### 4.4 Hydrogen adsorption weight percent and hydrogen adsorption energy for defective Pristine and Polycrystalline carbon nanotubes

Hydrogen adsorption weight percentage was determined for the defective pristine carbon nanotubes using the potential energy distribution patterns of  $H_2$  molecules are adsorbed around the CNTs at different pressure and at temperature 77 K , 100K and 200 K as shown in Figure 4.14 and here we can observed that due to defects in pristine carbon nanotubes containing 5, 7 and 8 member rings i.e. monovacancy defects hydrogen adsorption weight percentage is more than the non-defective carbon nanotubes because in defective carbon nanotubes it creates a gap between carbon atom due to monovacancy defects and due to this gap more hydrogen molecules are adsorbed in carbon nanotubes and also we can observed that hydrogen adsorbed wt % is increased with increasing percentage of defects in pristine carbon nanotubes.

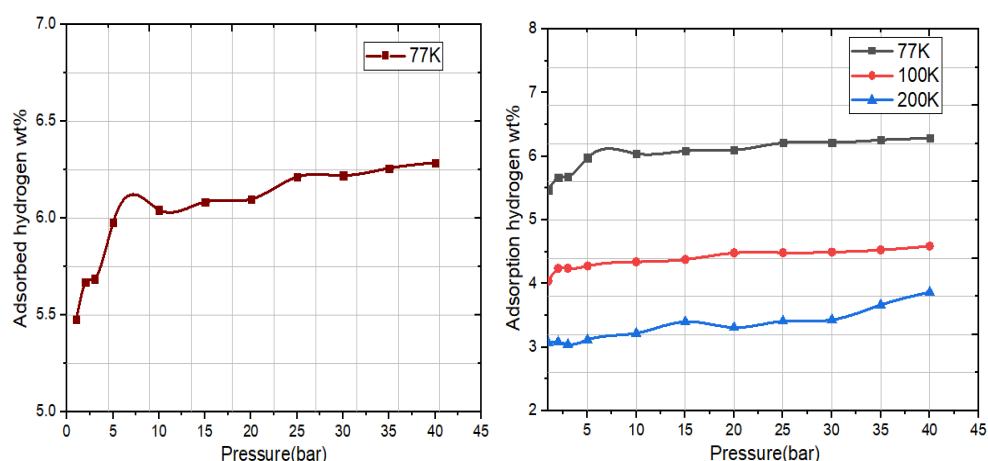


**Figure 4.14 Variation of hydrogen adsorption wt% for defective pristine carbon nanotube at different pressure at 77K and at different temperature.**

Adsorption hydrogen energy (ev) was determined using the data obtained for the defective pristine carbon nanotubes for hydrogen molecules for different pressure ranging from 1 bar to 40 bar and at 77K, 100K and 200K temperature as shown in Figure 4.15. Here we can see that the adsorption energies are calculated in negative values and adsorption energy is less as compare to pristine carbon nanotubes because there is formation of defects in pristine carbon nanotubes and due to these defects adsorption strength of hydrogen molecules is strong due to this adsorption energy is decreases. Higher value

adsorption hydrogen energy signifies a stronger attractive force between the adsorbate and adsorbent. If the pressure increases we can observed that the hydrogen adsorption energy reduces to a more negative value indicating that the stronger adsorption between the defective pristine carbon nanotubes and hydrogen molecules.

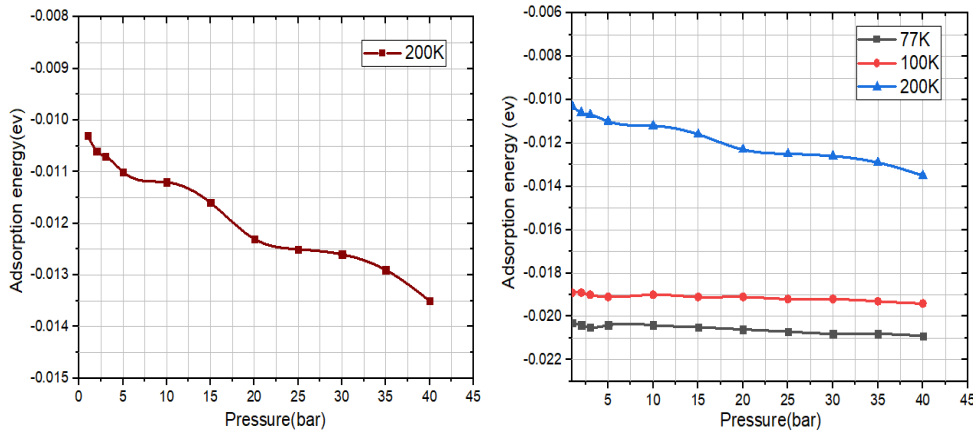


**Figure 4.15 Variation of adsorption hydrogen energy (ev) for defective pristine carbon nanotubes with different pressure at different temperature.**

Hydrogen adsorption weight percentage was determined for the defective polycrystalline carbon nanotubes using the potential energy distribution patterns of  $H_2$  molecules are adsorbed around the CNTs at different pressure and at temperature 77 K and 100K as shown in Figure 4.16(a) and here we can observed that due to defects in polycrystalline carbon nanotubes containing 5, 7 and 8 member rings i.e. monovacancy defects hydrogen adsorption weight percentage is more than the non-defective carbon nanotubes because in defective polycrystalline carbon nanotubes it creates a gap between carbon atom due to monovacancy defects and due to this gap more hydrogen molecules are adsorbed in polycrystalline carbon nanotubes and also we can observed that hydrogen adsorbed wt % is increased with increasing percentage of defects in polycrystalline carbon nanotubes.

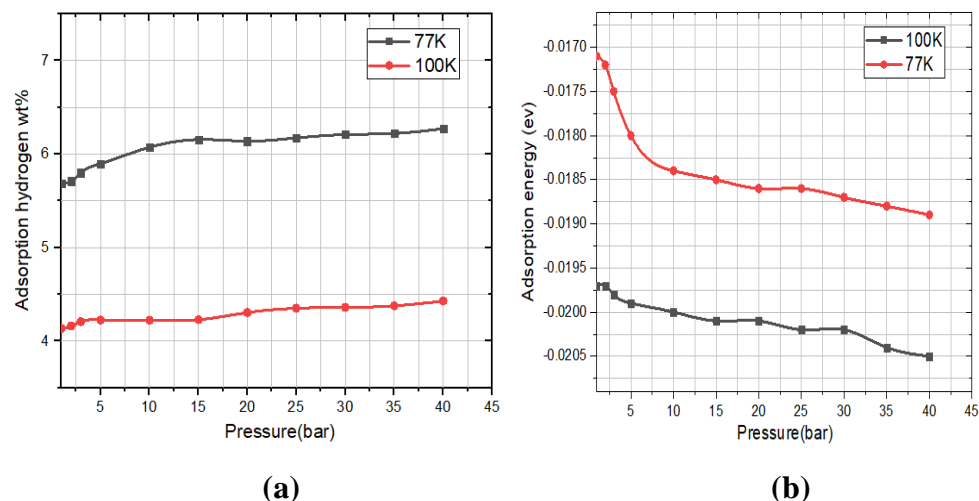


**Figure 4.16 Variation of (a) adsorption hydrogen wt% (b) hydrogen adsorption energy (ev) of defective polycrystalline carbon nanotubes with different pressure at 77K and 100K temperature.**

Adsorption hydrogen energy (ev) was determined using the data obtained for the defective polycrystalline carbon nanotubes for hydrogen molecules for different pressure ranging from 1 bar to 40 bar and at 77K and 100K temperature as shown in Figure 4.16(b). Here we can see that the adsorption energies are calculated in negative values and adsorption energy is less as compare to pristine carbon nanotubes because there is formation of defects in polycrystalline carbon nanotubes and due to these defects adsorption strength of hydrogen molecules is strong due to this adsorption energy is decreases. Higher value adsorption hydrogen energy signifies a stronger attractive force between the adsorbate and adsorbent. If the pressure increases we can observed that the hydrogen adsorption energy reduces to a more negative value indicating that the stronger adsorption between the defective polycrystalline carbon nanotubes and hydrogen molecules.

MDS simulations were performed to determine the hydrogen adsorption density and adsorption hydrogen energy (ev) for hydrogen molecules for both the pristine and polycrystalline carbon nanotubes for different temperature and pressure and also to determine the hydrogen adsorption density and adsorption hydrogen energy (ev) with considering the effects of strain in pristine carbon nanotubes at different temperature and pressure. For the polycrystalline carbon nanotubes the grain boundaries were created using voronoi tessellation and the adsorption density of carbon nanotubes containing grain boundaries was also determined using the same approaches. Potential energy distributions approaches is used to provide an accurate results of the number of adsorbed hydrogen molecules in carbon nanotubes. Not a single study is used to estimate the gravimetric density for the hydrogen molecules in carbon nanotubes using MDS simulations.

The operating temperature increases the hydrogen adsorption capacity decreases due to increase in thermal motion of hydrogen molecules and also we can see that at lower temperature van der waals interaction between hydrogen gas molecules and carbon nanotubes are very strong and as temperature increases the van der Waals interaction decreases and then due to the strong interaction forces hydrogen adsorption density of hydrogen molecules are higher at lower temperature.

The pressure increases the gravimetric hydrogen density increases because at a higher density of hydrogen molecules adheres to the adsorbent upon increasing the pressure. And as the pressure is increased the hydrogen gravimetric capacity increases rapidly but after reaching a certain pressure value it reaches a saturation level.

The hydrogen adsorption density of carbon nanotubes containing grain boundary is more than that of the pristine carbon nanotubes because of grain boundary creating in carbon nanotubes than there is formation of some defects in carbon nanotubes and due to these defects hydrogen molecules are adsorbed more as compare to pristine carbon nanotubes.

## Reference

1. Iijima, Sumio; Ichihashi, Toshinari (17 June 1993). "Single-shell carbon nanotubes of 1-nm diameter". *Nature*. 363 (6430): 603–605. Bibcode:1993Natur.363..603I. doi:10.1038/363603a0. S2CID 4314177.
2. Bethune, D. S.; Kiang, C. H.; De Vries, M. S.; Gorman, G.; Savoy, R.; Vazquez, J.; Beyers, R. (17 June 1993). "Cobalt-catalyzed growth of carbon nanotubes with single-atomic-layer walls". *Nature*. 363 (6430): 605–607. Bibcode:1993Natur.363..605B. doi:10.1038/363605a0.
3. M. N. Nahas and M. Abd-Rabou, "Finite element modeling of carbon nanotubes," *Int. J. Mech. Mechatronics Eng.*, vol. 10, no. 3, pp. 19–24, 2010.
4. M. R. Davoudabadi and S. D. Farahani, "Investigation of vacancy defects on the young's modulus of carbon nanotube reinforced composites in axial direction via a multiscale modeling approach," *J. Solid Mech.*, 2010.
5. R. Ansari, M. Mirnezhad, and S. Sahmani, "Prediction of chirality- and size-dependent elastic properties of single-walled boron nitride nanotubes based on an accurate molecular mechanics model," *Superlattices Microstruct.*, vol. 80, pp. 196–205, 2015.
6. N. M. Anoop Krishnan and D. Ghosh, "Chirality dependent elastic properties of single-walled boron nitride nanotubes under uniaxial and torsional loading," *J. Appl. Phys.*, vol. 115, no. 6, 2014.
7. Lehigh, E. M.; Palumbo, G.; Lin, P.; Brennenstuhl, A. M. (1997-05-15). "On the relationship between grain boundary character distribution and intergranular corrosion". *Scripta Materialia*. **36** (10): 1211–1218. doi:10.1016/S1359-6462(97)00018-3. ISSN 1359-6462
8. C. Ataca, E. Aktürk, S. Ciraci, and H. Ustunel. High capacity hydrogen storage by metallized graphene. *Applied Physics Letters*, 93(4):043123, 2008.
9. M. Kunowsky, J. P. M. Lozar, and A. L. Solano. Material demands for storage technologies in a hydrogen economy. *Journal of Renewable*

- Energy, 2013 (878329):1-16, 2013.
10. D. Y. Goswami and F. Kreith. Energy Efficiency and Renewable Energy Handbook, Second Edition. CRC Press, 2015.
  11. R. B. Gupta. Hydrogen Fuel: Production, Transport, and Storage. CRC Press, 2008.
  12. P. L. Spath, M. K. Mann, and W. A. Amos. Update of hydrogen from biomass-determination of the delivered cost of hydrogen. Technical report, National Renewable Energy Laboratory, 2003.
  13. G. K. Thomas and M. O. Joan. Assessment of hydrogen-fueled proton exchange membrane fuel cells for distributed generation and cogeneration. In Proceedings of the 2000 U.S. DOE Hydrogen Program Review, 2000.
  14. M. M. Mench. Fuel Cell Engines. John Wiley & Sons, Inc., 2008.
  15. G. Zhang and S. G. Kandlikar. A critical review of cooling techniques in proton exchange membrane fuel cell stacks. International Journal of Hydrogen Energy, 2012.
  16. M. Kunowsky, J. P. M. Lozar, and A. L. Solano. Material demands for storage technologies in a hydrogen economy. Journal of Renewable Energy, 2013.
  17. J. Yang, A. Sudik, C. Wolverton, and D. J. Siegel. High capacity hydrogen storage materials: attributes for automotive applications and techniques for materials discovery. Chemical Society Reviews, 2010.
  18. [https://www.assignmentpoint.com/science/chemistry/compressed-hydrogen.html\[comp\]](https://www.assignmentpoint.com/science/chemistry/compressed-hydrogen.html[comp]).
  19. A. C. Dillon and M. J. Heben. Hydrogen storage using carbon adsorbents: past, present and future. Applied Physics A, 72(2):133-142, 2001.
  20. Zacharia R, Rather S. Review of solid state hydrogen storage methods adopting different kinds of novel materials, J Nanomater 914845 (2015).
  21. Schlapbach L, Züttel A. Hydrogen-storage materials for mobile applications, Nature 414, 353-8 (2011).
  22. Moradi, R. and Groth, K. M. (2019) 'Hydrogen storage and delivery:

- Review of the state of the art technologies and risk and reliability analysis', *International Journal of Hydrogen Energy*. Elsevier Ltd, pp. 12254–12269. doi: 10.1016/j.ijhydene.2019.03.041.
23. Rivard, E., Trudeau, M. and Zaghbi, K. (2019) 'Hydrogen storage for mobility: A review', *Materials*. MDPI AG. doi: 10.3390/ma12121973
  24. Dai L. *Intelligent macromolecules for smart devices: from materials synthesis to device applications*. 1st ed. Berlin: Springer-Verlag; 2004.
  25. Barghi, S. H., Tsotsis, T. T. and Sahimi, M. (2014) 'Chemisorption, physisorption and hysteresis during hydrogen storage in carbon nanotubes', *International Journal of Hydrogen Energy*, 39(3), pp. 1390–1397. doi: 10.1016/j.ijhydene.2013.10.163.
  26. Baughman RH, Zakhidov AA, De Heer WA.(2002) Carbon nanotubes the route toward applications. *Science* 2002; 297:787-92. <http://dx.doi.org/10.1126/science.1060928>.
  27. Surya VJ, Iyakutti K, Mizuseki H, Kawazoe Y.(2011) First principles study on desorption of chemisorbed hydrogen atoms from single-walled carbon nanotubes under external electric field. *Int J Hydrogen Energy* 2011; 36:13645-56.
  28. Bastos-Neto, M. et al. (2012) 'Assessment of hydrogen storage by physisorption in porous materials', *Energy and Environmental Science*. Royal Society of Chemistry, 5(8), pp. 8294–8303. doi: 10.1039/c2ee22037g.
  29. Chambers, A. et al. (1998) 'Hydrogen storage in graphite nanofibers', *Journal of Physical Chemistry B*. doi: 10.1021/jp980114l.
  30. Gu, C. et al. (2001) 'Simulation study of hydrogen storage in single walled carbon nanotubes', *International Journal of Hydrogen Energy*. Pergamon, 26(7), pp. 691–696. doi: 10.1016/S0360-3199(01)00005-2.
  31. Lee, S. M. et al. (2000) 'Hydrogen adsorption and storage in carbon nanotubes', *Synthetic Metals*. Elsevier Sequoia SA, 113(3), pp. 209–216. doi: 10.1016/S0379-6779(99)00275-1.
  32. Nishimiya, N. et al. (2002) 'Hydrogen sorption by single-walled carbon nanotubes prepared by a torch arc method', *Journal of Alloys and Compounds*. Elsevier, 339(1–2), pp. 275–282. doi:

10.1016/S0925-8388(01)02007-2.

33. Takagi, H., Hatori, H., Yamada, Y., et al. (2004) 'Hydrogen adsorption properties of activated carbons with modified surfaces', *Journal of Alloys and Compounds*. Elsevier, 385(1–2), pp. 257–263. doi: 10.1016/j.jallcom.2004.03.139.
34. A. C. Dillon, K. M. Jones, T. A. Bekkedahl, C. H. Kiang, D. S. Bethune, and M. J. Heben. Storage of hydrogen in single-walled carbon nanotubes. *Nature*, 386:377-379, 1997.
35. P. Benard and R. Chahine. Determination of the adsorption isotherms of hydrogen on activated carbons above the critical temperature of the adsorbate over wide temperature and pressure ranges. *Langmuir*, 17(6): 1950-1955, 2001.
36. F. Darkrim and D. Levesque. Monte carlo simulations of hydrogen adsorption in single-walled carbon nanotubes. *The Journal of Chemical Physics*, 109(12):4981-4984, 1998.
37. F. Darkrim and D. Levesque. High Adsorptive Property of Opened Carbon Nanotubes at 77 K. *The Journal of Physical Chemistry B*, 104(29):6773- 6776, 2000.
38. E. Poirier, R. Chahine, P. Benard, D. Cossement, L. Lafi, E. Melancon, T. K. Bose, and S. Desilets. Storage of hydrogen on single-walled carbon nanotubes and other carbon structures. *Applied Physics A*, 78(7):961-967, 2004.
39. Y.L. Chen, B. Liu, J. Wu, Y. Huang, H. Jiang, and K.C. Hwang. Mechanics of hydrogen storage in carbon nanotubes. *Journal of the Mechanics and Physics of Solids*, 56(11):3224-3241, 2008. ISSN 0022-5096.
40. F. Darkrim and D. Levesque. Monte carlo simulations of hydrogen adsorption in single-walled carbon nanotubes. *The Journal of Chemical Physics*, 109(12):4981-4984, 1998.
41. N. Nasruddin, E. A. Kosasih, B. Kurniawan, S. Supriyadi, and I. A. Zulkarnain. Optimization of hydrogen storage capacity by physical adsorption on open-ended single-walled carbon nanotube as diameter function. *International Journal of Technology*, 7(2), 2016.
42. R. F. Cracknell. Simulation of hydrogen adsorption in carbon



- nanotubes. *Molecular Physics*, 100(13):2079-2086, 2002.
43. F. Darkrim and D. Levesque. High Adsorptive Property of Opened Carbon Nanotubes at 77 K. *The Journal of Physical Chemistry B*, 104(29):6773-6776, 2000.
  44. Y. Ye, C. C. Ahn, C. Witham, B. Fultz, J. Liu, A. G. Rinzler, D. Colbert, K. A. Smith, and R. E. Smalley. Hydrogen adsorption and cohesive energy of single-walled carbon nanotubes. *Applied physics letters*, 74(16):2307-2309, 1999.
  45. Q. Wang and J. K. Johnson. Optimization of Carbon Nanotube Arrays for Hydrogen Adsorption. *The Journal of Physical Chemistry B*, 103(23): 4809-4813, 1999.
  46. J. Cheng, X. Yuan, L. Zhao, D. Huang, M. Zhao, L. Dai, and R. Ding. GCMC simulation of hydrogen physisorption on carbon nanotubes and nanotubes arrays. *Carbon*, 42:2019-2024, 2004.
  47. L. Guo, C. Ma, S. Wang, H. Ma, and X. Li. Molecular simulation of hydrogen adsorption density in single-walled carbon nanotubes and multilayer adsorption mechanism. *Journal of Materials Science & Technology*, 21(1): 123-127, 2005.
  48. Juarez-Mosqueda R, et al. Theoretical analysis of hydrogen spillover mechanism on carbon nanotubes, *Frontiers in Chem A* 3, 2 (2015).
  49. W. Liu, Y. H. Zhao, Y. Li, Q. Jiang, and E. J. Lavertnia. Enhanced hydrogen storage on Li-dispersed carbon nanotubes. *The Journal of Physical Chemistry C*, 113:2028-2033, 2009.
  50. E. Rangel, J. M. Ramirez de Arellano, and L. F. Magana. Variation of hydrogen adsorption with increasing Li doping on carbon nanotubes. *Phys. Status Solidi B*, 248:1420-1424, 2011.
  51. P. Chen, X. Wu, J. Lin, and K. L. Tan. High H<sub>2</sub> uptake by alkali-doped carbon nanotubes under ambient pressure and moderate temperatures. *Science*, 285(5424):91-93, 1999.
  52. R. T. Yang. Hydrogen storage by alkali-doped carbon nanotubes-revisited. *Carbon*, 38(4):623-626, 2000.
  53. Ghosh S, Padmanabhan V. Hydrogen storage in Titanium-doped single-walled carbon nanotubes with Stone-Wales defects, *Diam Relat Mater* 77, 46-52 (2017).

54. Alian, A.R., Meguid, S.A. and Kundalwal, S.I., 2017. Unraveling the influence of grain boundaries on the mechanical properties of polycrystalline carbon nanotubes. *Carbon*, 125, pp.180-188.
55. Kun Xue and Zhiping Xu. Strain effects on basal-plane hydrogenation of graphene: A first-principles study. *Appl. Phys. Lett.* 96, 063103.
56. Shikai Deng, Anirudha V. Sumant, Vikas Berrya. Strain engineering in two-dimensional nanomaterials beyond graphene, *Nano Today*, 1748-0132 (2018).
57. Surya VJ, Iyakutti K, Mizuseki H, Kawazoe Y. Modification of graphene as active hydrogen storage medium by strain engineering, *Comput Mater Sci* 65, 144–148.
58. Miao Zhou, Yunhao Lu, Chun Zhang, and Yuan Ping Feng. Strain effects on hydrogen storage capability of metal-decorated graphene: A first-principles study, *American Institute of Physics*, 103109 (2010). [doi:10.1063/1.3486682]
59. K. S. Novoselov, A. K. Geim, S. V. Morozov, D. Jiang, Y. Zhang, S. V. Dubonos, I. V. Grigorieva, and A. A. Firsov, *Science* 306, 666 (2004).
60. K. S. Kim, Y. Zhao, H. Jang, S. Y. Lee, J. M. Kim, J. H. Ahn, P. Kim, J. Y. Choi, and B. H. Hong, *Nature (London)* 457, 706 92009).
61. C. Lee, X. D. Wei, J. W. Kysar, and J. Hone, *Science* 321, 385 (2008).
62. F. Guinea, M. I. Katsnelson, and A. K. Geim, *Nat. Phys.* 6, 30 (2010).
63. K. Xue and Z. P. Xu, *Appl. Phys. Lett.* 96, 063103 (2010).
64. M. Zhou, A. Zhang, Z. Dai, Y. P. Feng, and C. Zhang, “Strain-enhanced stabilization and catalytic activity of metal nanoclusters on graphene,” *J. Phys. Chem. C* (to be published), DOI: 10.1021/jp105368j.
65. Stone A. J. and Wales D. J. Theoretical studies of icosahedral C<sub>60</sub>, and some fuzlated species. *Chemical Physics Letters*, 128:501-503, 1986.
66. P. G. Collins. Defects and disorder in carbon nanotubes. *Oxford Handbook of Nanoscience and Technology: Frontiers and Advances*, 2010.
67. V. Gayathri and R. Geetha. Hydrogen adsorption in defected carbon nanotubes. *Adsorption*, 13:53-59, 2007.

68. C. H. Chen and C. C. Huang. Enhancement of hydrogen spillover onto carbon nanotubes with defect feature. *Microporous and Mesoporous Materials*, 109(1-3):549-559, 2008.
69. C. H. Chen and C. C. Huang. Hydrogen adsorption in defective carbon nanotubes. *Separation and Purification Technology*, 65(3):305-310, 2009.
70. Plimpton, S. 'Fast parallel algorithms for short-range molecular dynamics', *Journal of Computational Physics*. Academic Press, 117(1), pp.1-19. doi:10.1006/jcph.1995.1039.
71. M. P. Allen and D. J. Tildesley, "Computer Simulation of," *Liq.* Oxford Univ. Press. New York, vol. 18, no. 195, p. 385, 1987.
72. Y. Jin and F. G. Yuan, "Simulation of elastic properties of single-walled carbon nanotubes," *Compos. Sci. Technol.*, 2003.
73. H. Sun, "Ab Initio Calculations and Force Field Development for Computer Simulation of Polysilanes," *Macromolecules*, 1995.
74. Thesis Modeling and simulation of Boron Nitride Nanotube using Lammmps Software 04-07-2018.
75. Y. Jin and F. G. Yuan, "Simulation of elastic properties of single-walled carbon nanotubes," *Compos. Sci. Technol.*, 2003.
76. Klechikov, A. G. et al. (2015) 'Hydrogen storage in bulk graphene-related materials', *Microporous and Mesoporous Materials*. Elsevier, 210, pp. 46–51. doi: 10.1016/j.micromeso.2015.02.017.
77. Momma, K. and Izumi, F. (2011) 'VESTA 3 for three-dimensional visualization of crystal, volumetric and morphology data', *Journal of Applied Crystallography*. International Union of Crystallography, 44(6), pp. 1272–1276. doi: 10.1107/S0021889811038970.
78. Tersoff, J. (1989) 'Modeling solid-state chemistry: Interatomic potentials for multicomponent systems', *Physical Review B*. American Physical Society, 39(8), pp. 5566–5568. doi: 10.1103/PhysRevB.39.5566.
79. Bu, H. et al. (2009) 'Atomistic simulations of mechanical properties of graphene nanoribbons', *Physics Letters, Section A: General, Atomic and Solid State Physics*. North-Holland, 373(37), pp. 3359–3362. doi: 10.1016/j.physleta.2009.07.048.

80. Cracknell, R. F. (2001) 'Molecular simulation of hydrogen adsorption in graphitic nanofibres', *Physical Chemistry Chemical Physics*. The Royal Society of Chemistry, 3(11), pp. 2091–2097. doi: 10.1039/b100144m.
81. Langmuir, I. (1918) 'The adsorption of gases on plane surfaces of glass, mica and platinum', *Journal of the American Chemical Society*. American Chemical Society, 40(9), pp. 1361–1403. doi: 10.1021/ja02242a004.
82. Freundlich, H. (1907) 'Über die Adsorption in Lösungen', *Zeitschrift für Physikalische Chemie*, 57U(1), p. 385–470. doi: 10.1515/zpch-1907-5723.
83. Sips, R. (1948) 'On the structure of a catalyst surface', *The Journal of Chemical Physics*, 16(5), pp. 490–495. doi: 10.1063/1.1746922.
84. Fritz, W. and Schluender, E. U. (1974) 'Simultaneous adsorption equilibria of organic solutes in dilute aqueous solutions on activated carbon', *Chemical Engineering Science*. Pergamon, 29(5), pp. 1279–1282. doi: 10.1016/0009-2509(74)80128-4.
85. Ophus C, Shekhawat A, Rasool H, Zettl A. Large-scale experimental and theoretical study of graphene grain boundary structures, *Phys Rev B* 92, 205402 (2015).
86. Huang et al. Grains and grain boundaries in single-layer graphene, *Nature* 469, (7330) 389-392 (2011).
87. Lamari, F. D. and Levesque, D. (2011) 'Hydrogen adsorption on functionalized graphene', *Carbon*. Elsevier Ltd, 49(15), pp. 5196–5200. doi: 10.1016/j.carbon.2011.07.036.